T.C.
FATIH UNIVERSITY
INSTITUTE OF BIOMEDICAL ENGINEERING

DIAGNOSIS OF LEPTOMENINGEAL METASTASES DISEASE BY USING IMAGE ENHANCEMENT METHODS

MEHMET GÜL

Ph.D. THESIS
BIOMEDICAL ENGINEERING PROGRAMME

ISTANBUL, DECEMBER / 2015

T.C.
FATIH UNIVERSITY
INSTITUTE OF BIOMEDICAL ENGINEERING

DIAGNOSIS OF LEPTOMENINGEAL METASTASES DISEASE BY USING IMAGE ENHANCEMENT METHODS

MEHMET GÜL

Ph.D. THESIS
BIOMEDICAL ENGINEERING PROGRAMME

THESIS ADVISOR
PROF. DR. SADIK KARA

İSTANBUL, DECEMBER / 2015

T.C.
FATİH ÜNİVESİTESİ
BİYOMEDİKAL MÜHENDİSLİK ENSTİTÜSÜ

LEPTOMENİNGEAL METASTAZ HASTALIĞININ GÖRÜNTÜ İYİLEŞTİRME METOTLARI KULLANILARAK TANISININ KONULMASI

MEHMET GÜL

DOKTORA TEZİ
BİYOMEDİKAL MÜHENDİSLİĞİ PROGRAMI

DANIŞMAN
PROF. DR. SADIK KARA

İSTANBUL, ARALIK / 2015

T.C.

FATIH UNIVERSITY

INSTITUTE OF BIOMEDICAL ENGINEERING

Mehmet GÜL, **a Ph.D.** student of Fatih University **Institute of Biomedical Engineering** student ID **620112008,** successfully defended the **thesis/dissertation** entitled "**Diagnosis of Leptomeningeal Metastases Diseases by Using Image Enhancement Methods**", which he prepared after fulfilling the requirements specified in the associated legislations, before the jury whose signatures are below.

____

Prof. Dr. Sadık KARA

Thesis Supervisor

____

Prof. Dr. Abdurrahman IŞIKDOĞAN

Co-Supervisor

Examining Committee Members

Prof. Dr. Sadık KARA __________________________

Fatih University

Assoc. Prof. Dr. Muhammed Ali KAPLAN __________________________

Dicle University

Asst. Prof. Dr. Niyazi KILIÇ __________________________

Istanbul University

Asst. Prof. Dr. Şükrü OKKESİM __________________________

Fatih University

Asst. Prof. Dr. Kadir TUFAN __________________________

Fatih University

It is approved that this thesis has been written in compliance with the formatting rules laid down by the Institute of Biomedical Engineering.

____

Prof. Dr. Sadık KARA

Director

To my dear family,

Date of Defense: **30 December 2015**

Date of Submission: **15 January 2016**

ACKNOWLEDGEMENTS

First, I would like to express my thanks to my advisor Prof. Dr. Sadık KARA for his excellent guidance, patience, vision, and motivation for doing this thesis. I have learned a lot from his experiences and academic studies. I would like to express my gratitude to Prof. Dr. Abdurrahman IŞIKDOĞAN and Dr. Yusuf YARAR for their participation in my thesis. I would like to thank assist. Prof. Dr. İsmail YILDIZ for statistical evaluation and radiologist technician Vahap BİLEN the technician of Radiology Department in Dicle University Hospitals for MRI database.

I also thank my instructors in the Institute of Biomedical Engineering for providing support. I special thanks for their endless patience, understanding, and encouragement to my big family (my mom, dad, brothers and sisters and also my wife) for their fully support.

December 2015 Mehmet GÜL

TABLE OF CONTENTS

Pages

CHAPTER 4

APPENDICES

LIST OF SYMBOLS

e	electron
cm	centimeter
ρ	density (kg/m^3)
c	speed of sound (m/sec)
T1/T2	Tesla
f(x, y)	input image
g(x, y)	output image
h(x, y)	operator
T[ ]	gray-level transformation function
r	pixel intensity
s	pixel intensity
h(x, y)	operator
H(u, v)	transfer function
c	constant
γ	gamma correction
$h(r_k)$	discrete function
n_k	number of pixels
k^{th}	intensity value
$p(r_k)$	probability of occurrence of intensity level
T(r)	single-valued
H^+	Hydrogen positive

ABBREVIATIONS

AFP	Alpha-Fetoprotein
ALL	Acute Lymphoblastic Leukaemia
AML	Acute Myeloid Leukaemia
BOS	Beyin-Omurilik Sıvısı
BPS	Bit-plane slicing
BT	Bilgisayarlı Tomografi
CEA	Carcinoembryonic Antigen
CM	Carcinomatous Meningitis
CNS	Central Nervous System
CSF	Cerebrospinal Fluid
CSI	Craniospinal Irradiation
CT	Computer Tomography
FDG	Fluorodeoxyglucose
Gd-MRI	Gadolinium Magnetic Resonance Imaging
GLS	Gray-level Slicing
INT	Image Negatives Transformation
LDH	Lactate Dehydrogenase
LM	Leptomeningeal Metastasis
LT	Logarithmic Transformation
MR	Magnetik Rezonans
MRI	Magnetic Resonance Imaging
MTX	Methotrexate
PDF	Probability Density Functions
PET	Positron Emission Tomography
PLT	Power-Law Transformations
PNS	Peripheral Nervous System
RT	Radiation Therapy
β-HCG	β-human chorionic gonadotrophin

LIST OF FIGURES

LIST OF TABLES

SUMMARY

DIAGNOSIS OF LEPTOMENINGEAL METASTASES DISEASE BY USING IMAGE ENHANCEMENT METHODS

Mehmet GÜL

Biomedical Engineering Program

Ph.D. Thesis

Advisor: Prof. Dr. Sadık KARA

Co-Advisor: Prof. Dr. Abdurrahman IŞIKDOĞAN

Meningeal layer consists of three layers and protects the brain and spinal cord and surrounds these parts. These layer are pia mater, arachnoid layer and dura mater. Pia and arachnoid layers seem to be a component of a two-layer structure called pia-arachnoid layer or leptomeninges. Dissemination of this disease is occurred to be in the advanced stages of some complicated cancers such as lung cancer, renal cell cancer, and etc. This metastasis is known as Leptomeningeal Metastasis (LM).

The tumors contaminate in the cerebrospinal fluid (CSF). The medical operation is more risky than other cancers. Consequently, diagnosis of LM is important. Different methods are used to diagnose LM disease such as CSF examination and imaging systems (Magnetic Resonance Imaging (MRI) or Computer Tomography (CT) examination).

In this thesis, some image enhancement methods were used. The probability of result of logarithmic transformation (LT) method and power-law transformation (PLT) method were almost the same and result was $p=0.000$ ($p<0.001$), and statistically high result was obtained. The sensitivity obtained from these two methods is 92.85% and specificity result is 71.42%. The sensitivity result is very high and also specificity result is high.

The probability of contrast stretching (CS) method was $p=0.031$ ($p<0.05$), and this result was statistically significant. The other four methods' results were insignificant. The sensitivity result obtained from CS method is 56.52% and specificity result obtained from CS method is 57.89%. These two results are not high enough the results obtained from LT and PLT methods.

In addition to this, second study is conducted and the obtained results are compared with the results of MRI images. The sensitivity of second study is 75% and the specificity result is 60.87%. The result obtained from images is closest to the results obtained from certain pathology results. If the subjects are increased, the result can be more precise.

Keywords: Magnetic Resonance Imaging, Computer Tomography, Cerebrospinal Fluid Examination, Chemotherapy, Radiotherapy, Leptomeningeal Metastases, Image Enhancement Methods, Logarithmic Transformation, Power-Law Transformation.

ÖZET

LEPTOMENİNGEAL METASTAZ HASTALIĞININ GÖRÜNTÜ İYİLEŞTİRME METOTLARI KULLANILARAK TANISININ YAPILMASI

Mehmet GÜL

Biyomedikal Mühendisliği Programı

Doktora Tezi

Danışman: Prof. Dr. Sadık KARA

Eş-danışman: Prof. Dr. Abdurrahman IŞIKDOĞAN

Meningeal katmanı üç katmandan oluşan ve beyni ve omurilik sistemini sarmalayıp koruyan bir yapıdır. Bu katmanlar pia mater, arachnoid mater ve dura mater'dır. Pia ve arachnoid mater katmanları beraber pia-arachnoid katmanını diğer adıyla leptomeningeal katmanını oluştururlar. Hastalığın yayılımı bazı kompleks kanser türlerinin ilerleyen aşamalarında kendini gösterir, bu kompleks hastalıklar akciğer kanseri, renal hücreli kanser, vb. Leptomeningeal katmanına yayılan bu kansere leptomeningeal metastaz (LM) kanseri denir.

Tümörler beyin-omurilik sıvısına (BOS) yayılım gösterir. Tıbbi müdahale diğer kanser gruplarına kıyasla daha risklidir. Diğer taraftan LM hastalığının tanısı bir o kadar önemlidir. LM hastalığının tanısı için birden farklı metot örneğin BOS sıvısı incelemesi, görüntüleme sistemleri (Magnetik Rezonans (MR) ya da Bilgisayarlı Tomografi (BT)) kullanılmaktadır.

Bu tezde, bazı görüntü iyileştirme metotları kullanıldı. Logaritmik dönüşüm (LD) ve güç kanunu dönüşümü (GKD) metotlarından elde edilen sonuçların olasılığı neredeyse birbirine yakın olmakla beraber, çok yüksek istatistik sonuç elde edilmiştir, $p=0.000$ ($p<0.001$). LD dönüşüm metodu ile elde edilen duyarlılık oranı 92.85% ve özgüllük oranı ise 71.42% dir. LD ve GKD metotlarından elde edilen duyarlılık oranı çok yüksek olmakla beraber özgüllük oranları da yüksek çıkmıştır.

Kontrast germe (KG) metodu ile elde edilen sonucun olasılığı $p=0.031$ ($p<0.05$), ve bu sonuç istatistiki olarak yüksektir. Kullanılan diğer dört metottan elde edilen sonuçlar önemsiz derecededir. KG metodu ile elde edilen duyarlılık oranı 56.52% ve özgüllük oranı ise 57.89% dir. KG metodu ile elde edilen duyarlılık ve özgüllük oranları LD ve GKD dönüşümlerinden elde edilen bu sonuçlar kadar yüksek değildir.

Yapılan bir diğer çalışma da ise LM hastalarının patoloji sonuçları ile iyileştirilmiş MR görüntüleri karşılaştırılmıştır. İkinci çalışmada ortaya çıkan duyarlılık oranı 75%, özgüllük oranı ise 60.87% dir. Görüntü iyileştirmeden elde edilen bu yüksek oran

patolojiden elde edilen kesin sonuçlara en yakındır. Çalışmanın denek sayısı artırılarak daha kesin bir sonuç elde edilebilir.

Anahtar Kelimeler: Manyetik Rezonans Görüntüleme, Bilgisayarlı Tomografi, Beyin Omurilik Sıvısı İncelemesi, Kemoterapi, Radyoterapi, Leptomeningeal Metastaz, Görüntü İyileştirme Metotları, Logaritmik Dönüşüm, Power-Law Dönüşümü.

CHAPTER 1

INTRODUCTION

Central nervous system (CNS) processes myriad information [1]. CNS consists of two structures; these are brain and spinal cord. The structure of CNS is protected by three-tier structure and the name of this structure is meninges. The top layer of meninges is dura mater, the middle layer is arachnoid mater and the bottom layer is pia mater. Arachnoid mater and pia mater are called together leptomenigeal layer [1, 2].

All three sublayers have different missions and different structures. Dura mater constitutes collagen fibers and is most thickest and durable layer. Arachnoid layer likes a spider web structures. It contains blood vessels which transmits the nutrients and exchange the waste matter. It also has subarachnoid layer. Pia mater is the thinnest layer and surrounds tightly CNS structure. It has holes occurred by blood vessels [3, 4].

Cerebrospinal fluid is circulated in the leptomeningeal layer especially in the subarachnoid layer and the mission of this fluid is protection and to act as a cushion for CNS system. The advanced cancer tumors can disseminate to other parts of organs in the body. If the tumor disseminate to leptomeningeal layer, the new cancer form is occurred [5].

Leptomeningeal metastases (LM) cancer occurs as a result of dissemination of cancer existing in the body. The tumor cells disseminate in the cerebrospinal fluid (CSF) and a new type of cancer is formed. This cancer type is more dangerous compared to other types of cancer in the body. LM which the medical operation is almost impossible was first diagnosed in 1870 [6].

Different types of cancer in the body can disseminate to the cerebrospinal fluid. The most common dissemination of cancer tumors occur in lung cancer patients. The result of dissemination of lung cancer tumor into cerebrospinal fluid is called leptomeningeal carcinomatosis [7, 8]. The disseminated tumors in the leptomeningeal layer are sometimes protected by immune system [9].

Cancer cells caused to LM disease spreads through in spinal fluid with the blood or cerebrospinal fluid [5]. Diffusion of tumor cells in leptomeningeal layer or subarachnoid layer spreads in different ways. These emissions are from the choroid plexus vessels or the arachnoid vessels hematogenous spread, direct extension of parenchymal or subarachnoid surface of cranial nerve perineural spread along the path takes the form [5, 10, 11].

Dissemination of primary tumors into leptomeningeal layer can be by hematogenous spread, direct spread, tumor moved from impaired venous plexus cover spread and etc. [12]. LM cancer is sometimes called different names because the characteristic of tumors disseminated in the CSF are different such as leptomeningeal melanomatosis, leptomeningeal carcinomatosis and etc. [9].

The tumor cells disseminated by different cancers in to CSF fluid have different shapes and sizes. The tumor cells adhering to leptomeningeal layer are sometimes poured in sufficient amounts into CSF fluid, as a result of this, CSF examination can be performed. In some cases, the amount of tumor cells are either poured into CSF fluid in sufficient quantity or are poured into CSF insufficient quantity and in this case LM cancer certainly cannot be diagnosed by CSF examination [12, 13].

Diagnosis of LM cancer is defined by CSF examination and medical image. The result of CSF examination is more accurate than the measurement obtained by the medical imaging system [14]. On the other hand, CSF examination has some disadvantages. For instance, the CSF fluid intake is more difficult and the result is obtained more lately than medical imaging system [15].

The medical images are obtained early. Whether the FLAIR MRI image or contrast-MRI image elicits the details. These MRI images obtain earlier than CSF examination but the MRI image results are not as certain as CSF examination result. When the tumor is disseminated to CSF fluid, the tumor cells are counted in the CSF fluid and this count gives us the exact result. Because of this reason, the CSF fluid examination is more certain than other diagnosis methods [8, 16].

The main purpose of this thesis is to explore the way of obtaining more precise and early results for diagnosis of LM cancer. For this purpose, we use image enhancement methods to get valuable results. As it is mentioned, LM disease is one of the most risky cancer type and the early diagnosis is extended life span and also improves the cancer patients’ life.

1.1 Purpose of Thesis

Cancer tumor disseminated into cerebrospinal fluid (CSF) is more dangerous than other cancer. In addition to this, the importance of leptomenigeal metastases (LM) cancer is increasing more and more every day because the possibility of medical operation compared to other types of cancer is almost impossible. Although early diagnosis of LM cancer increases overall survival time of cancer patients and also increases the life quality of cancer patients [14, 17].

CSF examination and imaging systems are used to diagnose LM cancer. Cell count and other materials analysis are carried out in the CSF fluid examination which is obtained from cancer patients. Cell counts increases the accuracy of the analysis performed. On the other hand, the feasibility of tumor areas are examined on the images obtained from magnetic resonance imaging system. If the tumor areas are selected on the MRI images, LM cancer can only be diagnosed [18, 19].

The main objective of this thesis is to provide faster and definitive diagnosis for LM cancer. Despite obtaining accurate results, the results of CSF fluid are obtained later and are made more difficult than MRI imaging system. In this study, the images obtained from MRI imaging system are intended to re-evaluate for more precise results.

High achievement obtained from in two different conducted studies scope of the thesis. In the first study, more than a thousand cancer patients’ records have been analyzed which admitted two state hospitals in Diyarbakır in the last decades and 42 LM cancer patients have been identified. The significant differences between the raw MRI images and MRI images of 42 LM cancer patients were trying to comprehend within the first scope study.

In the second study performed, 750 cancer patients’ records were examined, 33 patients’ records were received and these patients had both CSF examination and MRI images. The raw MRI images were with image enhancement methods and the results were compared with each other by particular a pathologist and a radiologist to perform the differences of results. In the both studies, the precise and early results have been intended to obtain within MRI imaging system instead of CSF examination.

1.2 Hypothesis

MRI images contain very rich information. The main point is to reveal the hidden details on the image. Image enhancement methods can be used to reveal the hidden details and also the successful results are possible to achieve with these used methods. Finding the right image enhancement method and the correct using of the method reveal the hidden details on the images.

CHAPTER 2

LITERATURE REVIEW

Studies on leptomeningeal metastases cancer have mainly been as case studies so far. Relatively few studies have been carried out for diagnosis of LM cancer and the development of LM cancer diagnosis methods. The most remarkable example of study in diagnosis of LM cancer is to compare obtained images of gadolinium- T1 weighted MRI and images of gadolinium- FLAIR MRI [4, 20].

T1 and T2 weighted axial, contrast- FLAIR and FLAIR axial un sequences and T1-weighted sequences are investigated in these studies. In one of study, T1 and FLAIR images have been compared with each other and cancer tumor area was easily pointed in contrast- FLAIR images of 12 patients with definite diagnosis given LM cancer by clinical examination in respect of T1 contrast- sequence.

LM cancer is not just diagnosed with Magnetic Resonance Imaging (MRI imaging) system, sometimes Computer Tomography (CT) imaging system is used for diagnosis [1]. Soft tissue is demonstrated clearly in MRI imaging system in respect of CT imaging system. In one of study, imaging system results have been compared with others and the tumor areas have been clearly determined in the results obtained from FDG PET and advanced MRI sequences imaging systems. On the other hand, the definite results can be obtained by CSF examination results and CT and MRI imaging system results [1, 3].

Few studies have been executed to re-evaluate the obtained images. In addition to this, the noise on images was intended to eliminate and improve medical image quality [2]. The noise removal is one of the method to reveal the hidden details. The unwanted data is removed by using noise removal method and only desired information is remained in the image. The details are able to be clearly interpreted in the re-evaluated images.

The definite diagnosis of LM cancer is obtained as a result of the CSF examination. CSF fluid fills the brain ventricles and subarachnoid space, it is colorless liquid and formed by cells in the choroid plexus. CSF fluid acts as a cushion for brain and spinal cord. CSF fluid volume circulating from brain ventricles into the subarachnoid space is about 120-180 ml. 4/5 of CSF fluid is located around the brain and 1/5 of CSF fluid is located around the spinal cord. The main task of CSF fluid is to provide nutritional support to the nervous tissue and remove waste materials. The structure of CSF fluid does not contain any cells and if there are any cells in the examined fluid, as in the study [16], LM cancer can be diagnosed by pathological evaluation. Diagnosis of LM cancer is obtained as a result of increment glucose levels in the CSF fluid examination.

2.1 Central nervous system

CNS is capable of processing myriad information and consists of brain and spinal cord; this information is sent to peripheral nervous system (PNS) during rest of the body [21]. PNS consists of ganglia and all nerves spread throughout the body except the brain and spinal cord, the principal task of the PNS is to provide communication between organs and limbs with CNS (Figure 2.1).

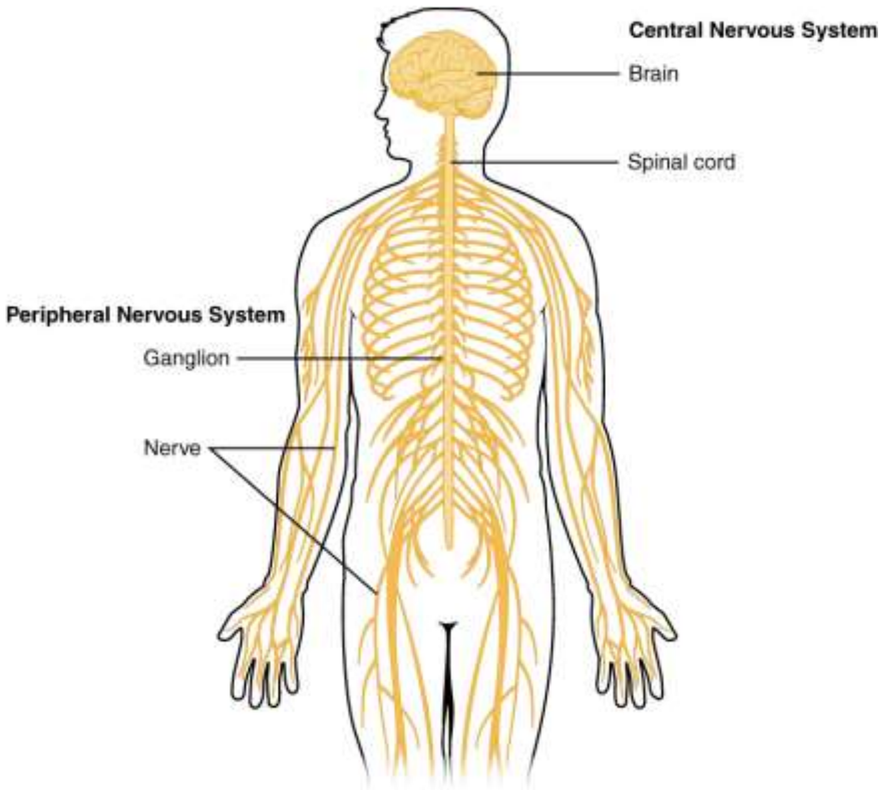

Figure 2.1 Peripheral nervous system (PNS)
(http://drsreejithnkumar.blogspot.com.tr/2015/05/myth-brain-stimulation.html 04/04/2015)

The CNS is surrounded the three-tier structure covers Latin expression meaning the meninges are used. Meninges structure consists of dura mater, arachnoid mater, and pia mater layers. These structures together acts as a cushion for the brain and spinal cord and they support the associated vascular structures. Meninges protect the brain three-layer structure is firmly joined to the inside of the skull and so that each side of the brain is encapsulated [22]. Meninges structure only in four different locations on the spinal cord has a loose structure [21].

2.2 Dura Mater

Dura mater constituted of collagen fibers is the thickest and durable layer of the meningeal layers and this layer is closest to the skull [23, 24]. It is composed of two layers, the periosteal layer – attached to the skull and inner meningeal layer – and is closer to the brain. Dura mater consists of sinus vein-like structure, these structures are provided with clean blood flow to the brain's needs, and then the blood vessels in the pia mater by capillaries transmit blood flow to the brain (Figure 2.2). Around dura mater is located the physiological space between itself and the backbone, known as the epidural space. This range is only a few mm wide and surrounds the dura all the way down the spine from the foramen magnum to the tip of the sacrum [21, 22].

2.3 Arachnoid Mater

Arachnoid word as meaning is the name given to a structure with a spider web, located in the middle meningeal, is attached to the Dura mater layer and this layer serves to cushion impact to the CNS (Figure 2.2). In the Dura mater layer, sometimes some areas are occurred like sinuses formed. This protected structure is also called arachnoid granulation or arachnoid villi. Arachnoid layer does not take the shape of the folds of the brain; it looks like a loosely fitting sac. Arachnoid layer which is adjacent to the CSF fluid that they use a common area is called the subarachnoid space [24 – 26].

2.4 Subarachnoid Space

The flow of cerebrospinal fluid produced in all ventricular within the subarachnoid space occurs in a particular order. CSF fluid to flow in subarachnoid space fills the entire region. This region is located between the arachnoid mater and pia mater layers

(Figure 2.2). From fourth subarachnoid ventricular cerebrospinal fluid flow towards the surface occurs and the flow takes places here the entire outer surface of the brain and the spinal cord system [21 – 24].

2.5 Pia Mater

Pia mater is very fragile and the thinnest innermost structure of meningeal layer. Pia mater surrounds tightly all around both brain and spinal cord and extends to the curved inner structure of the brain (Figure 2.2). Membrane layer is composed very thin fibrous tissue and surface is covered with squamous cell lengthways. This property has given liquid repellency. There are holes in pia mater for blood vessels leading to the brain and spinal cord [7, 24]. Arachnoid mater and the pia mater are usually together known as leptomeninges and have a common embryonic structure.

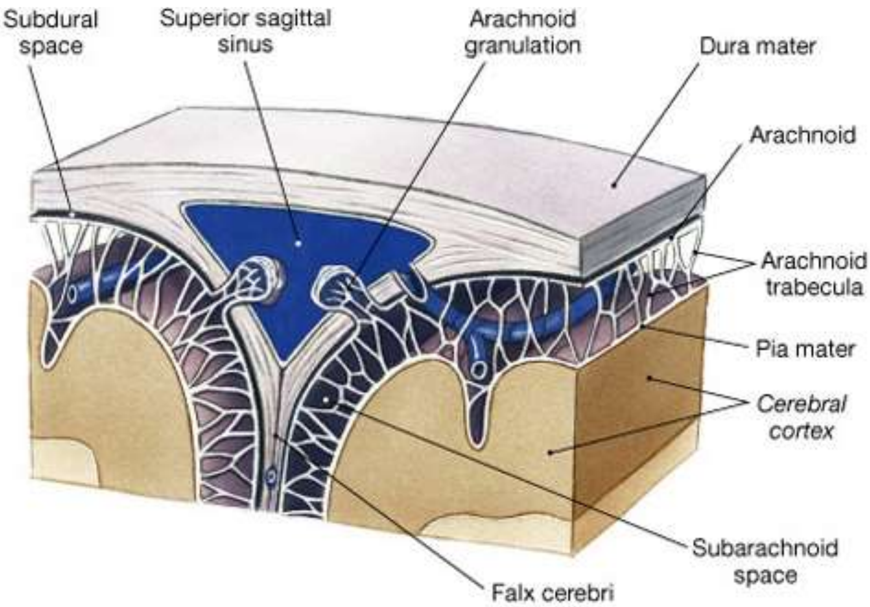

Figure 2.2 Open form of meningeal layer (http://droualb.faculty.mjc.edu/Lecture%20Notes/Unit%205/chapter_15_the_brain%20Spring%2007with%20Figures.htm 04/04/2015)

2.6 Choroid Plexus

All ventricles have choroid plexuses structures, with this construction, the formation of blood and cerebrospinal fluid in the ventricles of structure manufacturing is performed. The pia mater forms the choroid plexuses [24].

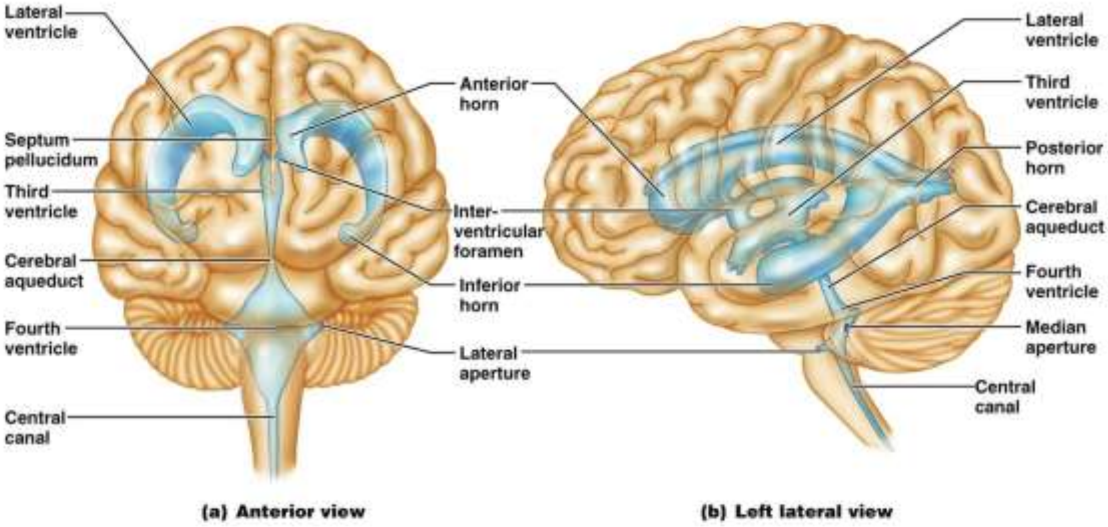

Figure 2.3 Ventricles of the Brain
(http://webs.ashlandctc.org/mflath/Brain%20and%20Cranial%20Nerves%20Lab%20PPT-VIEW.pdf 04/04/2015)

2.7 Ventricles

Ventricles have like stem-cell in order and their task produces new neurons. The new cells produced here migrate to places previously determined. Ventricles are filled by cerebrospinal fluid and these structures are composed of four regions (Figure 2.3). Ventricles communicate with the subarachnoid space. These structures also protect the brain as well as act as a cushion for the brain compensates for the weight of the brain [24].

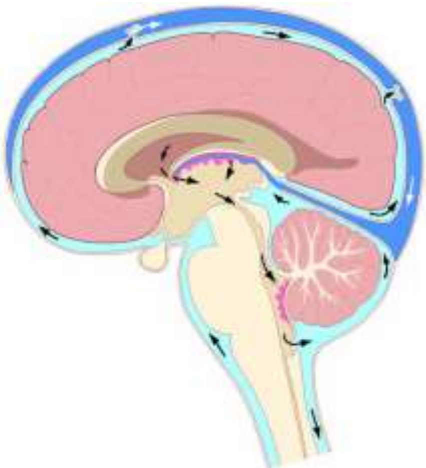

Figure 2.4 Circulation of CSF fluid
(http://energydynamics.ch/behandlung/cranio/ 04/04/2015)

2.8 Cerebrospinal Fluid

Cerebrospinal fluid (CSF) is colorless, transparent and a plasma ultra-filtrate liquid. This liquid rate of about 50-70% of the choroid plexus in the ventricles within the brain are produced by altered ependymal cells (Figure 2.4). Remaining parts of this fluid is produced around the blood vessels or in the walls of the ventricles. Cerebrospinal fluid transports nutrients, chemical messengers and waste products.

Cerebrospinal fluid contains little protein and few cells. However the presence of blood in cerebrospinal fluid is always abnormal. CSF fluid circulates in the subarachnoid space. As blood is filtered by the saliva, for neuraxis and cortex structure acts as cushion or buffer, and makes the flow of the nutrients needed for brain and spinal cord also throws out waste material from the system.

The human brain weighs about 1400 grams, this weight corresponds about 50 grams in cerebrospinal fluid served as a cushion for the brain [11, 12]. CSF fluid is filtered again by the blood through arachnoid granulations.

CSF fluid has four basic tasks. These are:

a) Buoyancy: The average human brain is 1400 grams, but in the CSF fluid the brain weight is equivalent to a mass of 50 grams. On the other hand the brain is in neutral buoyancy, this structure is in the task of protecting of intact brain under its own weight.

b) Protection: CSF protects brain tissue from damage during vibration or shock. Such as in automobile accidents or sports injuries in some cases, cerebrospinal fluid cannot protect the brain from the skull impact and sometimes even death can result in these situations.

c) Chemical stability: cerebrospinal fluid flows through the ventricular structures of the brain, transmits the nutrients that brain tissue needs and helps to remove the waste material occurred in the brain tissue.

Protection of brain ischemia: protection of brain ischemia occurs in a limited space inside the skull when there is a decrease in the amount of CSF fluid. This event reduces the pressure inside the skull and facilitates blood perfusion.

2.9 Leptomeningeal Metastasis

Angiogenesis plays an active role in the growth of tumors, such that growth and development of tumor cells spread to 2 mm^3 [9, 18]. Medical intervention of tumors contaminated CNS is great risks. Leptomeningeal Metastasis (LM) also known as carcinomatous meningitis is a type of cancer caused by tumor cells contaminated to CNS. First, in 1870, the case had been reported by Eberth in a patient with lung cancer, by then it had been considered a rare condition and could be diagnosed only at autopsy. It had been considered a rare condition and could be diagnosed only at autopsy [5, 13].

Diffusion of tumor cells in leptomeningeal layer or subarachnoid layer spreads in different ways. These emissions are from the choroid plexus vessels or the arachnoid vessels hematogenous spread, direct extension of parenchymal or subarachnoid surface of cranial nerve perineural spread along the path takes the form [27 – 29]. Sometimes, tumor cells can use to protect from the body’s immune system [30]. Some types of complicated cancer spread to leptomeningeal layer of brain and spinal cord, CNS tumors such as medulloblastoma or ependymoma tumors, disseminate within craniospinal leptomeningeal layer axis observed between 10% and 30% of cancer patients [6, 31, 32].

Solitary tumors of LM patients is observed in a high rate of 4-15%, rate of 5-15% blood cancer patients such as leukemia and lymphoma and rate of 1-2% brain metastasis patients [6, 31]. Tumors of LM patients during autopsy are observed in microscopic or macroscopic sizes. Causes of disease formation are chemotherapy, other medical interventions for the treatment of cancer patients or fail the blood brain uptake, the blood-CSF and the brain-CSF barriers applications [27, 33]. Brain metastases treated and non-treated among individuals are similar and brain metastases are more common with the intrinsic biology of HER2 positive breast cancer cases [34, 35].

Primary tumors spread of the leptomeningeal layer is realized in different ways (Figure 2.5):

a) By hematogenous spread (spread is the most common)

b) Direct spread

c) Moved from impaired venous plexus cover spread

d) Through nervous spread

e) Perineural and perivascular through the lymphatic spread

f) Choroid plexus escape or through subependymal metastasis spread

g) Iatrogenic way (during parenchymal metastases surgery)

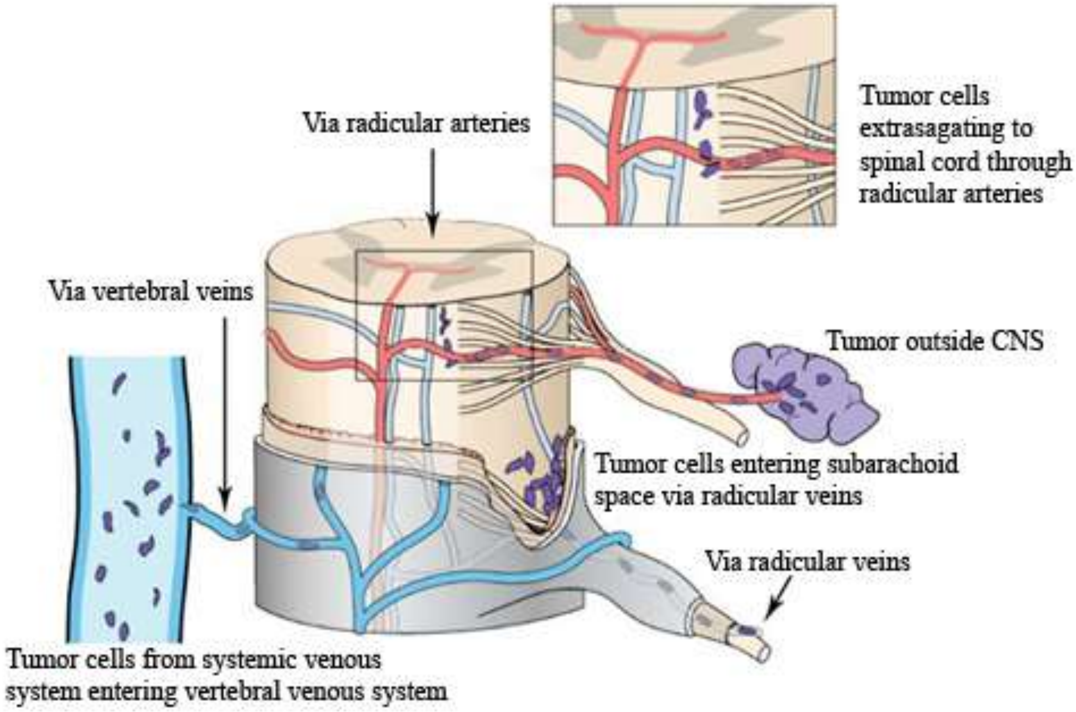

Figure 2.5 Perivascular Spread of Cancer Cells to Leptomeningeal Surface in Spinal Cord [36]

In the study, conducted in 2010, with about 60,000 of 70,000 results observed in cancer patients and LM disease were observed 16% of patients with lung cancer, 10% of patients with renal cell cancer, 7% of patients with melanoma, and in 1% of patients with colorectal carcinoma [19, 37, 38]. Some of the symptoms seen in patients with diagnosed brain metastasis are frequently were headache between 24% and 53%, focal weakness between 16% and 40%, altered mental status between 24% and 31%, seizures between 15% and 16%, and ataxia between 9% and 20% [39, 40].

Diagnosis of LM disease is challenging and a careful research or combination of clinical laboratory data, imaging systems and other tests need to be analyzed [30]. If tumors on brain sulci is not recognized, cerebellar folia and the cerebral sulci are seen typically because of that in MRI and CT images secondary appearance can be mistaken with intraparencymal metastases [41]. Early diagnosis of LM disease is more crucial for early initiation of treatment.

2.10 Diagnosis Methods

The brain tumor is examined in the laboratory tests. These tests are complete blood counts, electrolytes, renal and liver panels and etc. In addition to this, progression of primary or metastatic brain tumors are examined with images obtained from Computerized Tomography (CT) imaging system or Magnetic Resonance Imaging (MRI) system. In metastatic suspicion cases is required to examine lumbar puncture for CSF fluid analysis [15].

Especially in malignant cells spread in CSF fluid and on CNS various sites replicate. CSF fluid in cerebral ventricles and in subarachnoid layer between pia mater and arachnoid in other words leptomeningeal membranes also wraps around brain and spinal cord system. In addition to this, cancer cells are included within CSF fluid and CSF fluid can form secondary deposits in the leptomeningeal throughout the neuroxis [42].

Advances in diagnostic methods to be considered important by the day even more complicated is intended to facilitate the detection of biomarkers. The study conducted in 1980, the enzymatic activity of β-glucuronidase in the CSF fluid were detected. β-glucuronidase is tumor antigen, carcinoembryonic antigen and the detection of neoplastic meningitis has become easier [43]. Unfortunately, up to now no other antigen has been detected in any other antigens. According to this obtained antigen, today the detection of neoplastic meningitis has become easier.

2.10.1 Cerebrospinal Fluid Examination

Examination of cerebrospinal fluid (CSF) should be deliberated in the order parameters, the opening pressure, cell count, and protein and glucose count values. Based on these parameters during the observation of the disease can be diagnosed. For ideal examination of cytology of CSF fluid, while long needle is used anesthetic spray should be applied to the skin before operation (Figure 2.6).

Testing of biomarkers is another reference method for diagnosis of LM patients' disease, such as carcinoembryonic antigen (CEA), alpha-fetoprotein (AFP), β-human chorionic gonadotrophin (β-HCG), and monoclonal immunoglobulins elaborated [17]. Another method is used LM disease that other biomarkers are not fully defined to diagnosis, such biomarkers as β-glucoronidase, β-microglobulin and isoenzyme V of lactate dehydogenase (LDH) [27, 33]. Biomarkers generally are used for diagnosis of Leukemia and lymphoma, but other than these biomarkers and biomarkers non-inflammatory and/or infectious many acute or chronic processes are involving the leptomeninges [33].

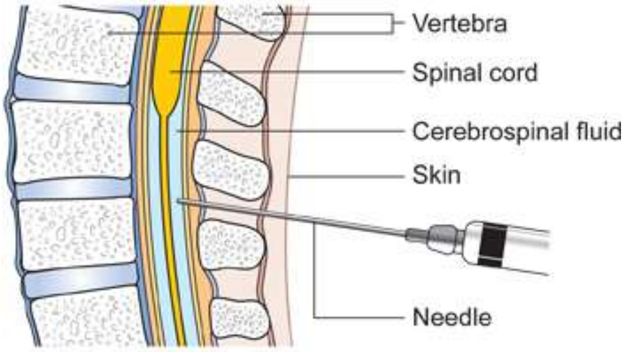

Figure 2.6 Obtaining cerebrospinal fluid
(https://www.scripps.org/articles/599-cerebral-spinal-fluid-csf-collection 04/04/2015)

When CSF fluid intake from patients, that occurs fear of having stroke, however such a possibility of stroke is one in a million. During process, respectively, the theoretical risks of CSF are listed as infection, local bleeding, nerve injury and brain herniation. Dizziness may occur after the procedure. For the treatment of these, the use of painkillers, bed rest and plenty of fluid intakes should be taken [44, 45].

Cytology of CSF plays an important role for the diagnosis of LM disease. However, in the study of Patchell et al. conducted on 54 patients who need biopsy, 11% of patients with glial tumor biopsy result, no result have been achieved, including abscess [46]. CSF cytology test repetition may result in increased sensitivity of diagnosis, the positive result is usually emerges in spread of tumor and as a sign of a deteriorating situation [47].

2.10.2 Imaging System

Imaging system especially, CT and MRI imaging systems are among the most commonly used methods for diagnosis of cancer patients. The early results as well as tumor location, tumor size and the amount of information are obtained with imaging systems. MRI imaging systems for the diagnosis of cancer is more preferred than CT imaging system. Especially with gadolium- multiplanar MRI images are obtained contrast- MRI images. Obtained contrast- images are provided more detailed and precise image than normal MRI images all the time [48]. While CT imaging system method acquires images with radiation exposure but MRI imaging system is not used radiation, because of this feature the use of MRI imaging system is more secure.

In the case of the CT imaging system, the CSF fluid must be sent to pathology and tested. Obstructive hydrocephalus must not ignore prior CSF fluid, otherwise under the CSF fluid is removed from the congestion in the process; the patient may be hernia or die. CSF fluid analysis has to be made on behalf of unnoticed condition on MRI images. If the disease is suspected, both methods have to be done for accurate diagnosis [49]. If there is any suspicious with patient's cranial nerve region, the images should be performed in thin sections.

Linear or nodular enhancement and thickening of lumbosacral roots of the cord may become visible with spinal MRI images. Patients with malignant solid tumor, hematologic tumor in LM patient's brain images is more likely to be abnormal [50]. A study on the sensitivity of MRI images, solid tumors and hematologic tumor has been seen in some of the contradictions between the images. This contradictory situation, while it is 90% of patients with solid tumors, this situation is observed 55% in leukemia patients [48, 51].

2.10.2.1 Computer Tomography Imaging System

Particularly, with X-ray radiation in CT imaging system is intended to elucidate the details of structures like blood perfusion of the brain (Figure 2.7). CT imaging system is shown to less developed regions of the brain, injured areas in any accident, tumors, lesions or infections [52]. Scanning brain with CT holds 30 minutes and patient is maintaining on the stretcher in horizontal position, meanwhile EEG device can be connected to patient to observe the heart rhythm and drugs can be injected to monitor patient vascular ways.

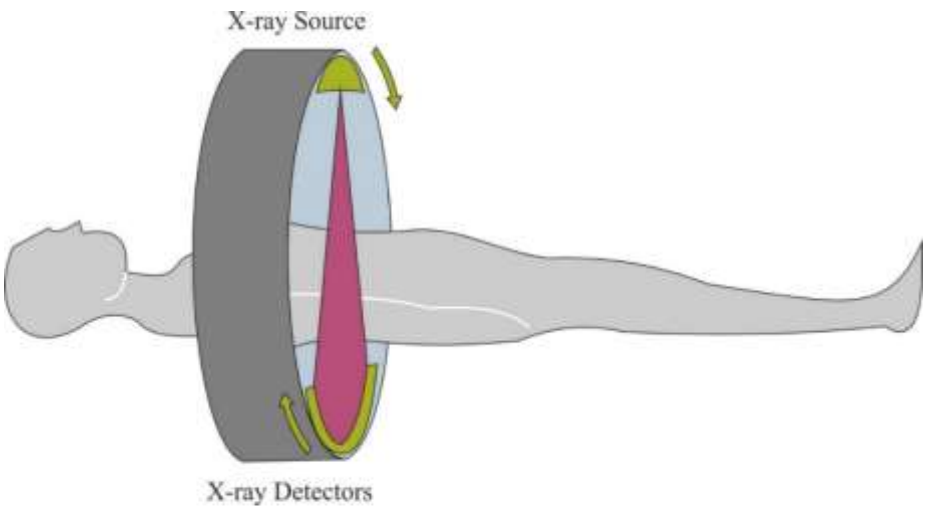

Figure 2.7 Working principle of CT process
(http://www.pf.bgu.tum.de/edu/pak/tum_pak_12_apfel_pre_sp2.pdf 04/04/2015)

2.10.2.2 Magnetic Resonance Imaging System

Magnetic Resonance Imaging (MRI) system takes picture of soft tissue of brain and other structures to the computer with strong magnetic field and radio waves (Figure 2.8). Protons in hydrogen atoms in the soft tissue are listed by magnetic field [53]. MRI imaging system’s most important feature that distinguishes from other imaging system is that the contrast of soft tissue image would help to consolidate with better resolution and sensitivity [54].

Drugs such as gadolinium are injected to the patient to obtain a more detailed contrast-MRI image of the patient. Another way to obtain the improvement image is to change the magnetic resonance signal strength. Primarily, tumors are evaluated by some groups, such as tumor vascularization and as to characterize flow properties by contrast-MRI images [55]. Not only tumors in specific area are displayed like in biopsy sample also displayed all tumors with functional MRI images [56].

MRI imaging is very important to be displayed to intracranial tumor. Pulses sequences, spin echoes or gradient echoes holds an important place for obtaining different T1 and T2 contrast with MRI imaging system in the tissue. Thus, the rest time, self-diffusion coefficients, laminar flow and other important physical properties are obtained with pulses sequences. Anatomical and functional properties can be defined as an important feature [56].

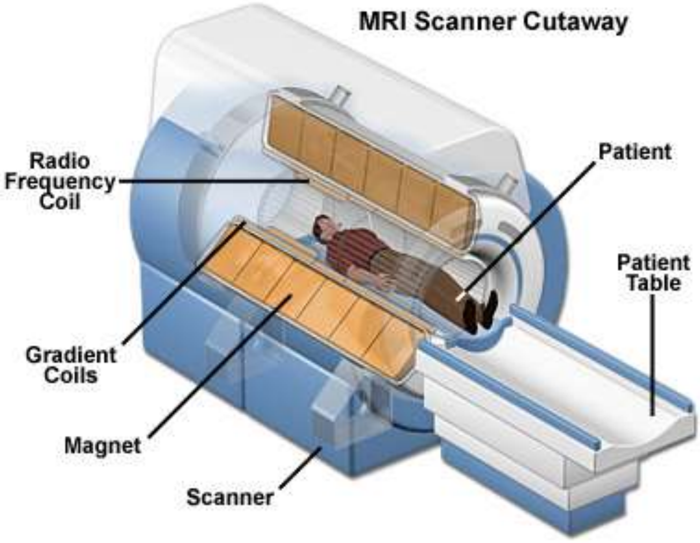

Figure 2.8 MRI imaging system
(http://ostenbarth.blogspot.com.tr/2013/06/como-funciona-ressonancia-magnetica.html 04/04/2015)

T1, T2 and T2* methods used in the MRI device demonstrate more detail of specific tissues in the brain [57]. For instance, tissue contain liquid or water is shown more brighter and while particulars are obtained more detailed, such hard structure as bone contain least liquid substances cannot be obtained detailed image. All methods are safe and painless used during MRI filming and radiation is not used, however, the marker injected into the patient may be able to provide different reaction [58].

A wide tube is required to create magnetic fields around the person for MRI scanning. The noise will occur during shooting, preferably it is attached music in headset or just headset and this period of process is completed around 15-40 minutes. If there is anything contented metal with patients they should be removed before processing of MRI filming; otherwise these metal contents are more dangerous. These metal implants can be inner ear implants, pacemaker, screws and etc. The patient can immediately continue their daily lives after MRI filming.

2.10.2.3 Differences of T1 and T2 MRI Machines

1.5 tesla machines is the first preferable device with high-field magnet features to get the most detailed or better resolution images by physician for diagnosis while the patients are examined less 20 – 30 min than 3 tesla machine [59]. 3 tesla machines generate twice as strong magnetic field in comparison with 1.5 tesla machine and strength of 1.5 tesla and 3 tesla machines produce more than 30.000 or 60.000 times magnetic field compared to earth magnetic field [60].

These valuable images have the property of 3 tesla MRI and it is used for pathological conditions involving the brain, spine and musculoskeletal system [61]. MRI imaging system is also demonstrated the common tissue. The brain structures are demonstrated with MRI in detail. The tissue appearances are disparity in T1 weighted and T2 weighted and STIR sequences. The signal intensities of T1 weighted MRI is different with the signal intensities of T2 weighted MRI.

2.10.2.4 Advantages of MRI Imaging System

MRI imaging system has some advantages. Patients entering the MRI machine are comforTable. Because open magnets creates a more comforTable situations for the patients. Sizes of units used in MRI imaging system are smaller. In other words, extremity units are smaller [62].

2.10.2.5 Disadvantages of MRI Imaging System

MRI imaging system has some disadvantages. When the machine is working, extreme precautions must be taken. At first, the metallic objects should be kept away from the room in which MRI is operating. Patients with cardiac disease especially patients has pacemakers in danger. Because device like pacemakers are affected by MRI magnetic fields. If people suffer from claustrophobia, they feel in discomforting situation. When MRI machine is working, it produces a very loud noise. The magnet size is in standard, thus some people may not be fit inside in magnet. The operating of MRI machine holds very long periods of time such as up to ninety minutes or more in some cases. MRI systems are too expensive [62].

2.10.2.6 Differences between CT and MRI Machine

Different conspicuously results are obtained When MRI imaging system is compared with CT imaging system, with MRI imaging systems accurate determination of the location of the lesion, the extend of lesion and especially small-sized lesions throughout the cerebral convex is showing more comforTable in this way.

The presence of calcification and bone abnormalities in CT imaging system are demonstrated more clearly compared with MRI imaging system such as degredation, erosion, permeability and hyperostosis. On the other hand, tumors, perifocal edema and the relationship between tumors and next structure are shown successful results in MRI imaging system compared with CT imaging system.

T2-weighted sequences have the most sensitivity to detect tumors and edema extend, on the other hand, tumor and edema are completely indistinguishable with this method. Such information as degree of tumor, blood-brain barrier breakdown, haermorrhage, edema and necrosis is usually detected in T1-weighted images. Contrast- T1-weighted images can also display small focal lesions, e.g. metastases, tumor recurrence small regions, ependymal and leptomeningeal spread of tumors. Proton concentration density of tissues helps to distinguish tumors and edema adjacent with CSF fluid [5].

Excellent contrast resolution images and multiplanar images of brain and spinal cord are obtained with contrast- MRI imaging system [41]. MRI imaging modalities used in the methods of cancer diagnosis, lesion distribution, to identify the number and the size is a more successful outcome compared to CT another imaging method of diagnosis of LM disease [44]. Because of the magnetic properties of MRI, MRI gets image by the movement and the density of hydrogen atoms of the soft tissue [63]. Due to these reasons, the referenced MRI method in diagnosing LM is one of the first methods and effects to display increment of LM occurrence [27, 33]. If any contradiction happens to take images of LM patients, myelography-CT imaging is used as an alternative.

Although there is not reached any common consensus about both imaging system, contrast- MRI images give 2-3 times more successful results compared to contrast- CT images, even including the ability to display lesions under 5 mm.

2.11 Treatment Methods

The main objectives of the treatment are that neurologic status is steadied or advanced and these treatments are extended the life-span. Systemic chemotherapy aims to maintain balance of cytotoxic concentrations of CSF fluids. Intra-CSF therapy is a treatment method used for treating CNS cancer and more particularly for the treatment of some cancers i.e. prophylactic potential. Four agents are used for intra-CSF therapy such as methotrexate (MTX), thiotepa, cytarabine, and liposomal cytarabine [38].

2.11.1 Chemotherapy

The main objective in the treatment of chemotherapy is to control neurological signs and to prevent tumors progression. Chemotherapy regimens fail to destroy tumors found in CSF fluid of LM patients [64, 65]. These drugs are more effective on sensitive tumor especially on breast cancer, germ cell, hematologic malignancies and small cell lung cancer [12, 30]. Four different chemotherapeutic agents in the treatment of intra-CSF is used i.e. methotrexate, thiotepa, cytarabine (Ara-C) and liposomal Ara-C [26]. Thin monolayer adherent cells in CSF fluid can only be treated with intra-CSF chemotherapy [66]. Clinical improvement are seen in cancer patients, if the patient' cytology results are negative, in this case with the same chemotherapy drugs should be continued consolidation and follow-up [10, 11].

2.11.2 Radiotherapy

Radiotherapy (RT) is a useful method in the treatment of great LM tumors, parenchymal brain metastases, sites of symptomatic disease or CSF flow obstruction [67]. Radiotherapy reduces the incidence of brain metastases that are LM cases of Lung cancer patient with small tumor cells, but not prevent relapse of leptomeningeal [12]. The pain in the method of radiotherapy indicates how this method is sensitive. LM disease is frequently occurring disease, although craniospinal irradiation (CSI) method can be used for the treatment [14].

2.11.3 Targeted Therapies

Targeted therapies nowadays, molecularly targeted therapies methods and the study of these methods are increasing with each passing day [26]. It is observed positive results from studies on the brain metastases induced non-small-cell lung carcinoma [68]. Particularly, the main purpose in different studies conducted in this area is to determine the location of the tumor region and eliminates the detected tumor cells.

CHAPTER 3

MATERIAL & METHOD

3.1 Data Acquisition

The data used in the study was taken from Dicle University Hospital Radiology Department and Diyarbakır Gazi Yaşargil Education and Research Hospital. In this thesis, there were 2 studies executed. In the first study, almost 1000 data were examined and 42 LM cancer patients were defined and 35 of 42 patients' records were obtained from Dicle University Hospital Radiology Department and the rest of data were obtained from Diyarbakır Gazi Yaşargil Education and Research Hospital. The property of the MRI images which are obtained from the 6 of the LM cancer patients are T1 weighted and the other ones are T2 weighted.

The first data used in the study was taken in 2014 and these records obtained between in 2003 and 2013 in two state hospitals. These records were obtained by examining almost 1000 patients' data in state hospitals. The second data used in the study was taken early in 2015 and these records obtained between in 2000 and 2015 in Dicle University Pathology Department. These records were obtained by examining about 750 patients' data in Dicle University Pathology Department. In the second study, 33 LM cancer patients' data were executed. The properties of all MRI images were T1 and T2 weighted axial, contrast- FLAIR and FLAIR axial un sequences and T1-weighted sequences. We intended to find LM patients, thus the diversity of data was not paid attention. The sample raw MRI images are shown in Figure 3.1.

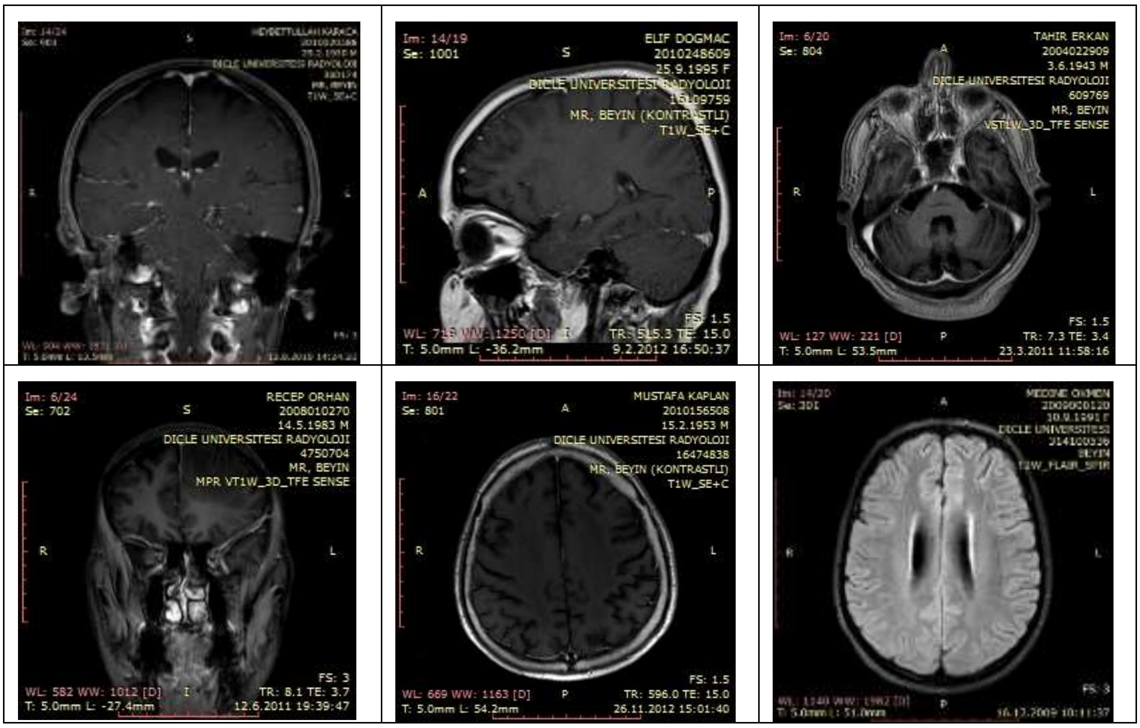

Figure 3.1 The samples of raw MRI images used in the study

These images belong to LM cancer patients and some of these images are demonstrated in Figure 3.1. These images are the LM patients’ raw MRI images. The images in the Figure 3.1 are DICOM format. As it is seen, patients’ all data are shown in the raw MRI images.

3.2 Image Process Methods

The main objective of image enhancement is that improves the image quality or reveals the hidden information for re-interpretation, for instance, in medicine for particular disease can be diagnosed by interpretation with captured image. There is not a general method in image enhancement; different methods are used according to the user’s request. The suitability of the image diagnosis is application dependent and success of enhancement is based on either that varies depending on the user subjectively or that varies depending on the set criteria.

Every detail on the image cannot be noticed by the eye. Vehicle from distance are not noticed, however such information of vehicle is transmitted to the brain as a car. These types of images are characterized by several criteria, such as low resolution, brightness and contrast, large mirror reflection and eyelid occlusion. Therefore, image enhancement leaves a mark that reveals the secret information on the image. Image enhancement both solves the problems of the image in digital media and improves the quality of the image. The image processing techniques are sharpening, smoothing, eliciting of tissue or analysis [59, 69].

Many methods are used in image enhancement. Main objective in all of these methods is to ensure that details on the images can be discerned. Validation rate of showing the best improvement in image enhancement methods are based on the law that sub-images in blurred images are filled with the nearest values. Other methods such as enhancement of sharpness and reduce noises for normalization are traditional histogram equalization, contrast enhancement, fuzzy masking and homographic filtration. Image enhancement methods are divided into two categories [59, 69].

- Frequency domain method
- Spatial domain method

In this study, it is aimed to diagnose the leptomeningeal metastases disease with image enhancement methods. Some of these methods give us proper results however the others give us unexpected results. The proper image results gotten from image enhancement methods are demonstrated in below.

3.2.1 Frequency domain method

The first step in the frequency domain is that image is transferred to the frequency domain [70]. Image enhancement with frequency domain method is based on convolution theorem and is formulated as follows:

$$g(x, y) = h(x, y) * f(x, y) \quad (3.1)$$

g(x, y) symbolizes output image, h(x, y) is operator and f(x, y) is defined as output image. If the above equation is rewritten in the Fourier Transform;

$$G(u, v) = H(u, v)\, F(u, v) \quad (3.2)$$

H(u, v) function acts as the transfer function equation

$$f(x,y) \;\rightarrow\; h(x,y) \;\rightarrow\; g(x,y) \quad (3.3)$$

$$F(u,v) \;\rightarrow\; H(u,v) \;\rightarrow\; G(u,v) \quad (3.4)$$

3.2.2 Spatial Domain Method

Spatial domain method is based on the pixels in the image and conversion of the pixel is performed such as point processing or mask processing [70, 71]. Pixels in the image are collected and these pixels values are changed to obtain the desired values. Spatial domain method is both more effective and uses fewer computer resources and allows fast processing. Spatial domain method usually creates three different effects on the image, respectively contrast and dynamic range modification, noise reduction and edge enhancement and detection. Spatial domain method can be shown with below process:

$$g(x,y) = T\ [f(x,y)] \tag{3.4}$$

f(x, y) input image, g(x, y) output image and T is an operation on the function f. T operator is applied each position (x, y) and the output value g is taken. In this case g function is based on f function according to value of (x, y) and form of function of T gray-level transformation:

$$r = f(x,y)\ s = g(x,y) \tag{3.5}$$

The value of g depends on f value; T: a gray-level transformation function

$$s = T\,(r) \tag{3.6}$$

r and s variables respectively is the grey surface variables obtained each (x, y) variables in f(x, y) and g(x, y) functions. r is pixel intensity of pre-processing and s is pixel intensity after processing.

The simplest form of T values is when taken as a neighbor has a value of 1 x 1, in other words, by taking the individual pixels (Figure 3.2). The transformation function compresses r value which is below m value and this compression is occurred into a narrow range of s, toward black [70]. In this case the used technique is also called contrast stretching method. In the Figure “a” is as shown in the graph. Whereas, in “b” Figure thresholding function is used to obtain two-dimensional binary image.

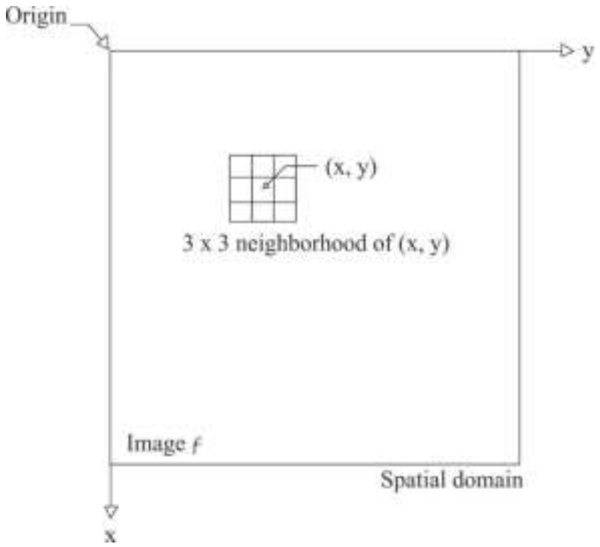

Figure 3.2 A 3 X 3 neighborhood about a point (x, y) in an image in the spatial domain (http://ceng503.cankaya.edu.tr/uploads/files/file/lecture2%281%29.pdf 04/04/2015)

Spatial domain method is divided in two categories; respectively Intensity transformation and spatial filtering. Intensity transformation contrast manipulation and image thresholding work on individual pixels on the image. Spatial filtering is related to the transactions carried out.

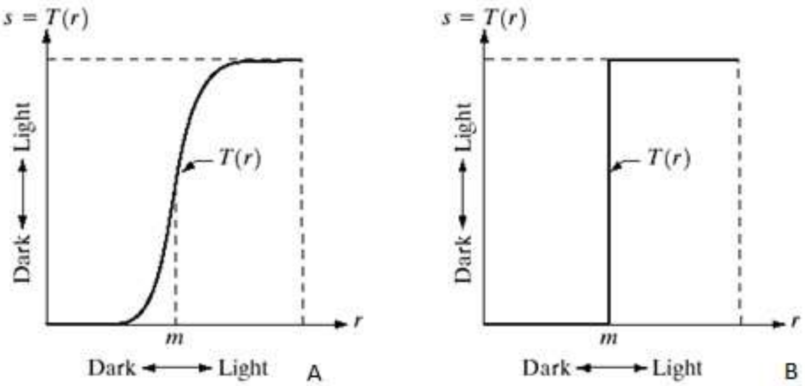

Figure 3.3 Gray-level transformation functions for contrast enhancement (http://opencvvision.blogspot.com.tr/ 04/04/2015)

3.2.2.1 Image Negatives Transformation

Image Negatives Transformation (INT method) method is the simplest and the most basic method in the image enhancement methods. The main aim of this image enhancement is to expand the white or the gray details embedded in dark areas on the image. Image negative: image negative with gray levels in the range of “0, L-1” (Figure 3.3).

s = L – 1 – r (3.7)

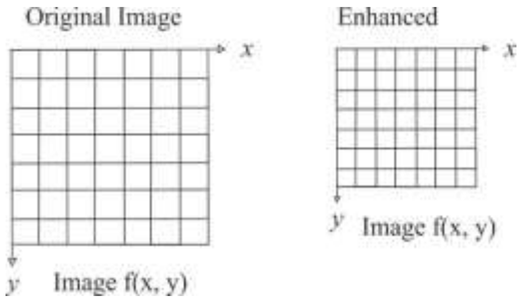

$$s = intensity_{max} - r \quad (3.8)$$

The format of processed image is 8-bit and extractions of the each pixel's value get made worth 255. M x N variables in the image is respectively symbolized that M is line and N is column and image is defined l(m, n) and negative image is defined g(m, n) based on f(m, n); the equation likes as following [71].:

$$g(m,n) = 255 - f(m,n) \begin{cases} 0 \leq m < M \\ 0 \leq n < N \end{cases} \quad (3.9)$$

When we applied image negative transformation method to MRI images used in the study, the intended results were not obtained. We used the "imcomplement" function to obtain the result. After applying this function to one of the sample MRI image used in the study is shown in Figure 3.4;

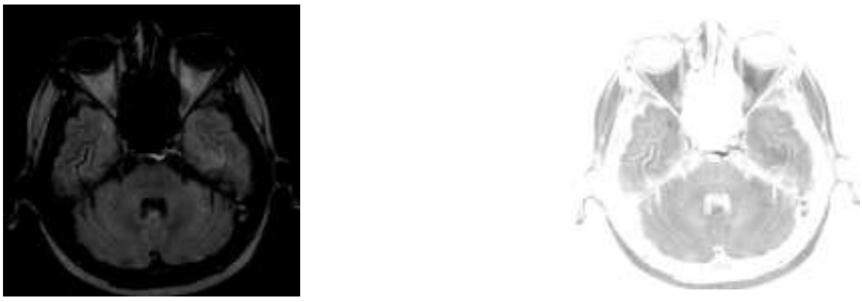

a) b)

Figure 3.4 Application of INT method to MRI images used in study. a) represents MRI image used in the study, b) represents by INT method

All pixels brightness in MRI image is increased equally with INT method and the eligibility of both the tumor contaminated into leptomeningeal layer and other peripheral tissues are decreased. In the Figure 3.4, a is represent the raw MRI image and b is represent the image by histogram processing.

The differences of these two images are distinctive. In the bright image only some surrounding tissue in the brain can be identified with uncertain. In some of INT method application, the satisfied results can be obtained such as the tumor in mammography image. On the other hand, the tumor in the leptomeningeal layer is not defined. Thus INT method is not suiTable for this study.

3.2.2.2 Thresholding Transformation

Thresholding method mainly gives effective results that distinguish different density tissue or different colored tissue above the background in image. The Figure 3.5 shows an example of this method applied. The image having bright colors on a dark background is defined as one-dimensional. The input of thresholding operations generally likes a color image or grayscale. Dark pixels symbolizes background, light-colored or white pixels symbolizes tissue or vice versa. Implementations are basically determined by threshold parameters. If the pixel density is greater than threshold value, the pixels are assigned the white value; if it is low; in that case pixels are assigned black value [72, 73].

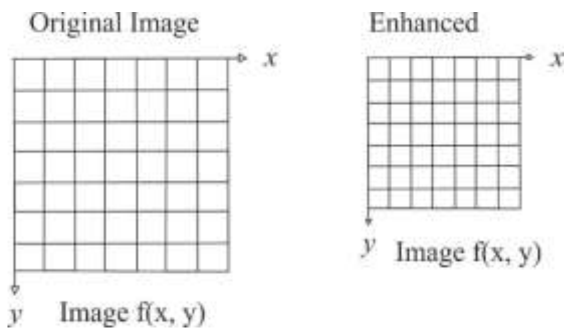

$$s = \begin{cases} 1.0 & r > threshold \\ 0.0 & r \leq threshold \end{cases}$$

When the thresholding method was applied on of the sample MRI image used in the study, unsatisfied results are obtained. We used graythresh function. First of all, we read the raw MRI image and used this function. After this, we used im2bw function to convert the raw image to binary image based on thresholding method. Finally, one of the results is shown in Figure 3.5;

a) b)

Figure 3.5 Application of thresholding transformation method to MRI images used in study. a) represents MRI image used in the study, b) represents by thresholding method

When we use thresholding method for diagnosis of leptomeningeal tumor, neither the tumor area in leptomeningeal layer is defined, nor is the surrounding tissue in the brain defined. In the Figure 3.5, a is represent the raw MRI image and b is represent the image by thresholding method. In the image the details are not eligible. Neither the tumor area is identified nor is surrounding tissue in the brain identified. For this reason, thresholding method is not suiTable for using this study.

3.2.2.3 Logarithmic Transformation

Logarithmic transformation is basic tool for dynamic range manipulation. Logarithmic transformation (LT) is based on remapping low gray level values into wider gray level values [74]. If a big amount of gray level values are in image, especially it would be more useful to use logarithmic transformation. The logarithmic transformation expands the dark pixels [70, 74]. LT looks like Gamma Transformation (Gamma<1) application [40]. Details are hidden in detail and rich content of the darkness of the area and thus the brightness value of each pixel are replaced with logarithmic values. The formula of logarithmic transformation is:

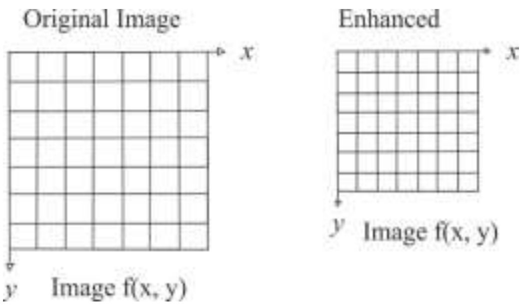

$$G = c * \log(1 + | r |) \qquad (3.10)\ [69]$$

c is a constant variable and r≥0. While the values of dark pixels are enlarging, a large level values are compressed with this transformation. Constant "c" value takes values between 0-255 in an 8-bit image; in other words, if R has a maximum value of the input image, in this case "c" variable is determined as follows.

$$c = \frac{255}{\log(1+|R|)} \tag{3.11}$$

Constant "c" takes maximum value of 255 in 8-bit image format. Brightness of the image is obtained by increasing the value of "c".

One of the best result for this study is taken from logarithmic transformation method. One of the sample MRI image used in the study was applied to this method. First of all, we converted the image into the double value and took the logarithmic function and multiply by 0.15 value. After these procedure, the obtained result is expected result and shown in the Figure 3.6.

When MRI image is by logarithmic transformation method, the radiologist notice the tumor area in this image. In the Figure 3.6, a is represent the raw MRI image and b is represent the image by LT method. The distinctive tumor area helps radiologist to diagnose LM cancer patient. We use the sample of MRI image, because the tumor area is eligible in this sample image and is recognized easily. Thus we use the same sample to demonstrate the differences of image enhancement methods for this study.

a) b)

Figure 3.6 Application of LT method to MRI images used in study. a) represents MRI image used in the study, b) represents by LT method

3.2.2.4 Power-Law Transformations

Power-law and piece-wise linear transformation methods want too much input from users [74]. Power-law transformation function is known gamma correction. Different results are obtained from different value from the variable γ, it is quite commonly called as Gamma Correction. In other words, each monitor returns the best image by adhering available images in a certain range of gamma in different ways to user [15]. The function used by power-law transformation method;

$$s = cr^{\gamma} \tag{3.12}$$

is defined, "c" and "γ" are the positive constants in functions. Gamma is written as top in power-law equation, power-law method uses the gamma correction for correction process. Sometimes, the equation emerges as $s = c(r + \varepsilon)^{\gamma}$. The graphics shown in the Figure 3.7 is generated by obtained reciprocal "s" and "r" variables depending on different "γ" values. Conversely logarithmic functions, possible transformation curves can be obtained with γ variable values [70].

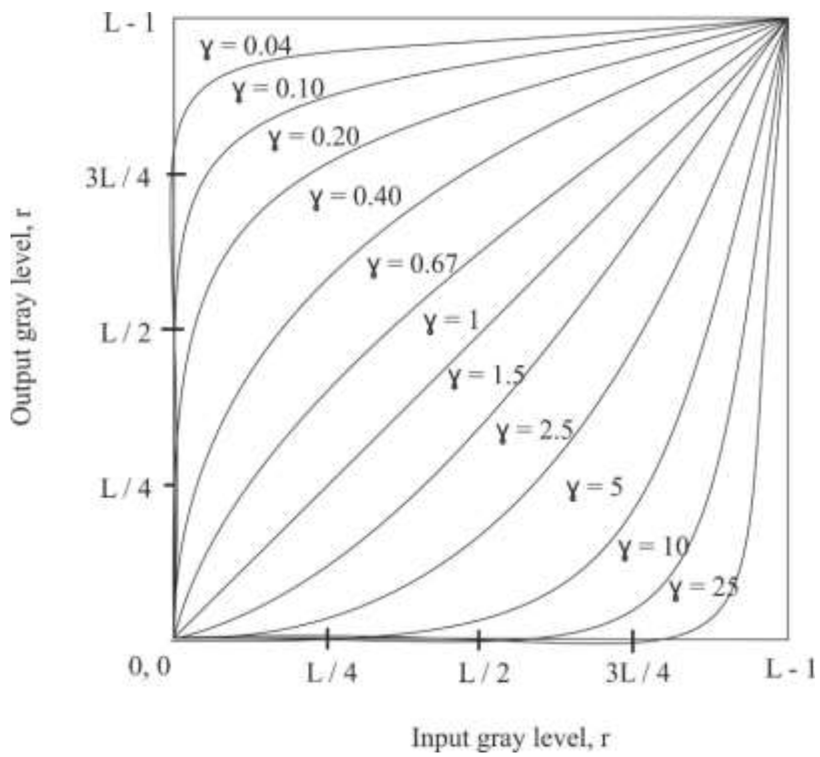

Figure 3.7 Power-law function curves
(http://www.slideshare.net/ASHI14march/enhancement-in-spatial-domain 04/04/2014)

If $\gamma < 1$, the narrow range of dark values are mapped into a wider range and bright pixel values are got wider ranges into a narrow range by power-law transformation.

If $\gamma > 1$, the opposite effects are occurred. Identity transformations occur if $c = \gamma = 1$ [74].

The detail in the MRI image of spinal cord was revealed more clearly in that sample. On the other hand, one of the sample MRI image used in the study was processed with this method and one of another best result was obtained. At first, after we opened the image, we converted the gray level image in RGB level, and then we convert the result of image to double. Finally, we check the image size and attend the size of image in two dimensions. We use c in equal to 2 and g in equal to 0.5. These variables were used in two "for" loops and then the MRI image is demonstrated in Figure 3.8.

In the Figure 3.8, a is represent the raw MRI image and b is represent the image by PLT method. The intended results were taken with power-law transformation method. This is because logarithmic transformation method actually likes using gamma transformation method (Gamma < 1). Power-law transformation method is known as gamma transformation method. Because of this, the results obtained from power-law transformation and logarithmic transformation method are unavoidably same.

a) b)

Figure 3.8 Application of PLT method to MRI images used in study. a) represents MRI image used in the study, b) represents by PLT method

3.2.2.5 Piecewise-Linear Transformation Functions

Piecewise-linear transformation functions can be complex and also piecewise functions can formulate some important transformations. Another advantages of this method is that piecewise functions can formulate some important transformations. On the other hand, users want more inputs compared to other conversions. This issue is the disadvantage of the method. Piecewise-linear transformation are divided into three;

- Contrast Stretching
- Gray-level Slicing
- Bit-plane slicing

3.2.2.5.1 Contrast Stretching Transformation

Contrast stretching transformations is the most basic piecewise-linear functions. If the rendered image is non-uniform lighting conditions, contrast stretching transformation is applied. This method performs broadening of the range of the intensity levels in the image [70].

For the obtained image “c” above.

$$(r_1, s_1) = (r_{min}, 0) \quad (3.13)$$

$$(r_2, s_2) = (r_{max}, L-1) \quad (3.14)$$

The equation formed for the obtained image “d”;

$$(r_1, s_1) = (m, 0) \quad (3.15)$$

$$(r_2, s_2) = (m, L-1) \quad (3.16)$$

m: mean gray level is considered (Figure 3.9).

a) b) c) d)

Figure 3.9 The application of CS transformation method. a) A low-contrast image, b) Result of contrast stretching, c) Result of thresholding, d) Form of CS transformation function
(http://www.slideshare.net/ASHI14march/enhancement-in-spatial-domain 04/04/2014)

The transformation function is shaped the position variables of r1, r2 and s1, s2;

- If $r_1 = s_1 \; and \; r_2 = s_2$, transformation linear is defined as a function and no chances are allowed.
- If $r_1 = r_2, s_1 = 0 \; and \; s_2 = L - 1$, transformation is defined as thresholding function and so that a binary image can be produced.
- If the median value of (r_1, s_1) and (r_2, s_2) variables is taken, spreading of gray layer of output image is produced at different levels.
- Usually, $r_1 \leq r_2 \; and \; s_1 \leq s_2$ are accepted.

Contrast stretching was applied to MRI images used in the study and although logarithmic transformation method and power-law transformation method have been obtained positive results. First, we used different values for obtained the best results. Thus we used stretchlim function, this function is investigated the stretch contrast of the image. Limits of the image are changed according to image contrast. For the best result, it is tried to change the contrast value. When we used the value of 0.18 and obtained the images. The sample image processed by contrast stretching method is demonstrated in Figure 3.10.

In the Figure 3.10, a is represent the raw MRI image and b is represent the image by CS method. The result is not as good as LT method and PLT method. This result resembles the histogram processing method. The results obtained from contrast stretching method are the most successful after the results obtained from the other two methods. The results are better than the results of raw MRI images.

a) b)

Figure 3.10 Application of CS method to MRI images used in study. a) represents MRI image used in the study, b) represents by CS method

3.2.2.5.2 Gray-Level Slicing

Gray-Level Slicing (GLS) method engages on the images which contains in a certain range of [A………B]. It is always intended to elicit something in a given tissue. For example, the desired image is revealed by the neglect of unwanted water stains on the images of X-ray from satellite imagery (Figure 3.11).

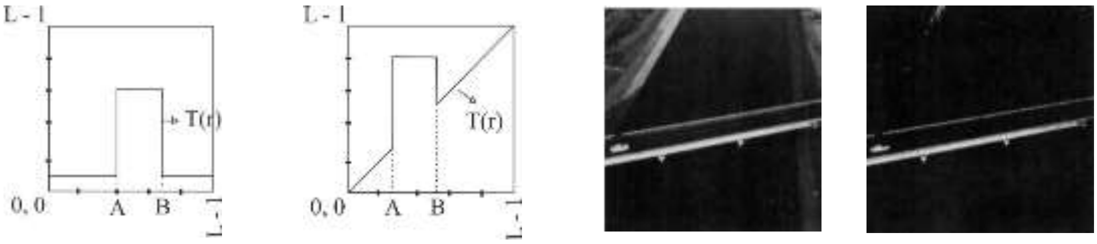

a) b) c) d)

Figure 3.11 The application of GLS method.
a) Highlighted in the range of [A, B], b) The all levels in range of [A, B], c) The original image. d) The processed image in a) by this transformation
(http://www.slideshare.net/ASHI14march/enhancement-in-spatial-domain 04/04/2014)

First the high gray values in the image put forward and the reduction of remainder values of all other gray is based on, the second is based on the transformation, while brightness of the desired range of gray tones is increased, background and other gray tones are protected. As an example of the first approach is shown in the “c” shape, the second approach is illustrated in the “d” shape shown as an example [70]. GLS method can be used to obtain different results, for this purpose the value of x and y dimension have to be arrange in proper situation. In this study, the image is, at first, converted in two dimension.

We need two “for” loop to appoint these two dimension in two different variables. After that, the first image x and y dimensions are checked and if these values are greater or equal than 90 and if these values are smaller or equal than 255, the designated area in the image and background are shown together. If it is not, just the designated area is shown alone. The sample MRI image used in the study was applied by gray-level slicing method and the results were not as expected. One of the results is shown in Figure 3.12;

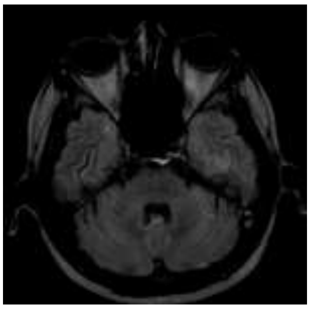

a)

b)

Figure 3.12 Application of INT method to MRI images used in study. a) represents MRI image used in the study, b) represents by GLS method

In the Figure 3.12, a is represent the raw MRI image and b is represent the image by GLS method. The details in this image is worse and almost none of the details can be identified. The all details of MRI images were almost lost and when this methods were applied, the results were not as expected. Due to the results, following conclusion can be reached that the gray-level slicing method is one of worse method for this study.

3.2.2.5.3 Bit-Plane Slicing

Pixels of images are comprised the digital numbers, in other words, the image can be defined as a sequence of numbers of bits with bit-plane slicing (BPS). Each image is formed from layers as in the Figure 3.13. The format of processed image lets it be accepted in 8-bits, in this case, form of images parts is considered in 1 bit and bit-plane are ranked from 0 to 7. Delamination of 8-bit image is represented in the following Figure.

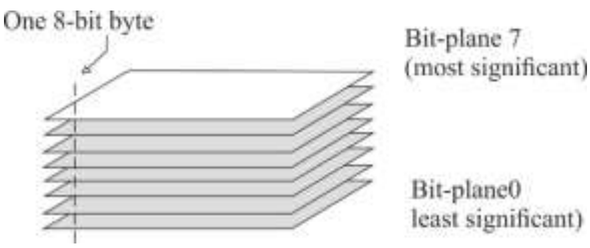

Figure 3.13 Delamination of image
(http://www.slideshare.net/ASHI14march/enhancement-in-spatial-domain 04/04/2014)

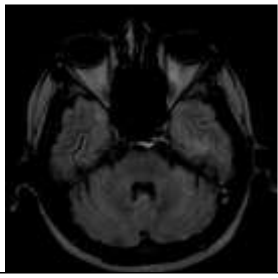			
The raw MRI image sample			
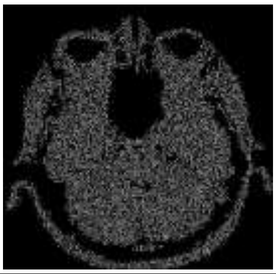	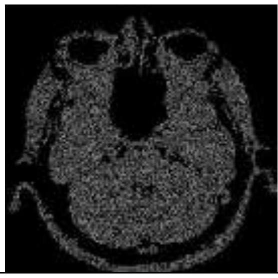	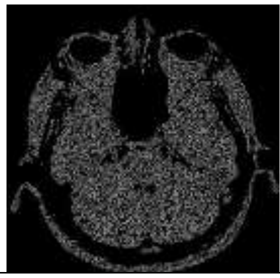	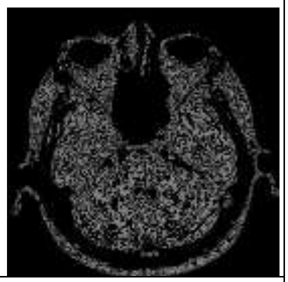
a) Bit-plane slicing = 1	b) Bit-plane slicing = 2	c) Bit-plane slicing = 3	d) Bit-plane slicing = 4
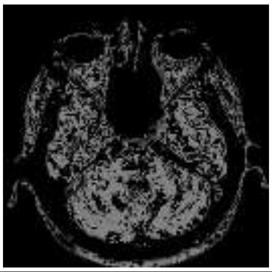	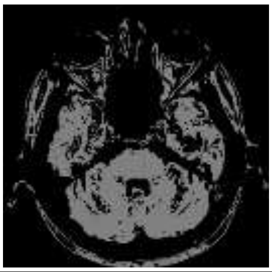	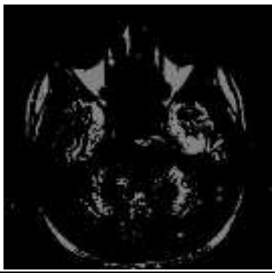	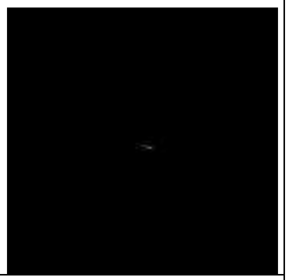
e) Bit-plane slicing = 5	f) Bit-plane slicing = 6	g) Bit-plane slicing = 7	h) Bit-plane slicing = 8

Figure 3.14 Application of bit-plane slicing method to MRI images used in study. Below images represents by bit-plane slicing method

The Figure 3.14 shows an 8-bit fractal image. The fractal image is derived from a mathematical equations and it is a multi-layered image [70]. First of all, we read the raw MRI image and then we check the size and appointed the size of image in two variable. We used two “for” loops and we used bitget and bitset functions in these “for” loops. After these we obtained the bit-plane images according to variables 1 to 8. Finally, one of the samples of MRI image used in the study are obtained with bit-plane slicing method and these results are shown in Figure 22. The raw MRI image and the other processed results obtained with bit-plane slicing method are shown together in Figure 22.

3.2.2.6 Histogram Processing

Histogram of the image symbolizes the association of the frequency occurrences of the different gray-levels in the image. Image is converted according to required specifications with histogram modeling techniques [72]. The discrete function of the histogram processing (HP) for the digital image is into the range of [0, L-1];

$$h(r_k) = n_k \tag{3.18}$$

k_{th} is the intensity value and also the r_k value is the k_{th} and n_k is the number of pixels in the image with intensity r_k. Total number of pixels in the image normalize and their values repeat with histogram process. Thus, normalized histogram equation is obtained that

$$p(r_k) = \frac{n_k}{MN} \text{ , } k = 0,1, \dots \dots \dots \dots L-1 \tag{3.19}$$

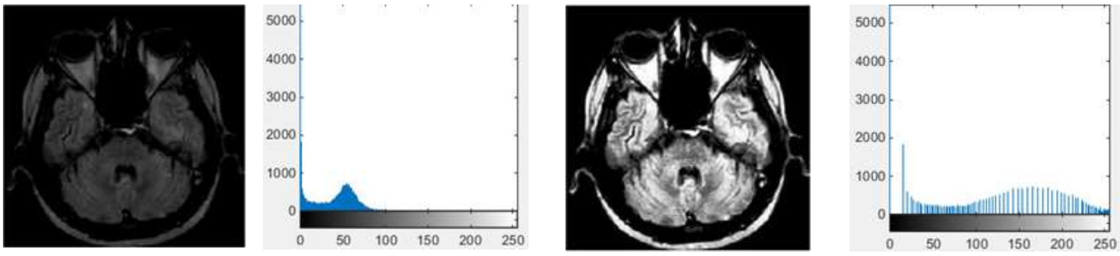

a) b) c) d)

Figure 3.15 Application of histogram processing method to MRI images used in study. a) original image used in the study, b) original image' histogram diagram, c) improved image by HP method, d) improved image' histogram diagram

"a" represents MRI image used in the study, "b" represents by histogram processing

The estimation of the probability of occurrence of intensity level r_k in the image can be seen $p(r_k)$. The horizontal axis of the histogram charts corresponds gray-level value that is r_k, if the vertical axis is normalized, it corresponds the value of $h(r_k) = n_k$ or $p(r_k) = n_k/MN$ [70].

The sample MRI image used in the study was applied by histogram processing method and the results were not as good as LT method or PLT method. The histogram functions we used are shown in Appendix B in detail and one of the results is shown in Figure 3.15;

The tumor area in this image is revealed however the results are not as good as LT method or PLT method and also the results of histogram is better than the results of CS method. The images shown in Figure 3.16, there are three different images and the raw image, these images are respectively obtained by histogram processing method, CS method and LT method.

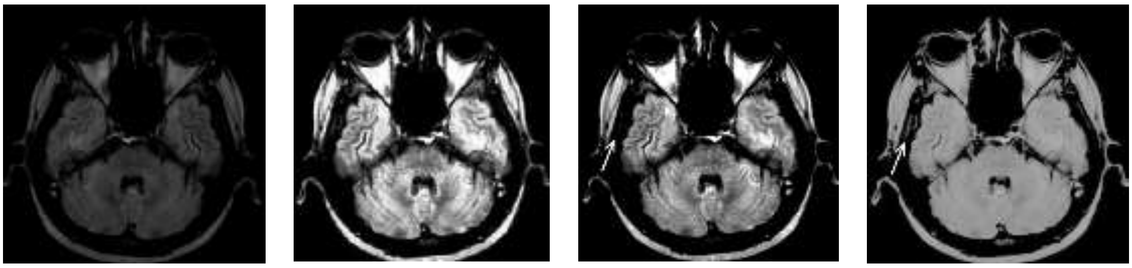

a) b) c) d)

Figure 3.16 Comparison of three different methods.
a) The Raw Image, b) Improved Image by HP, c) Improved Image by CS,
d) Improved Image by LT

CHAPTER 4

RESULTS

As it is known, MRI images store many details, but every detail are not displayed on MRI images and some details remain hidden in dark areas, such as LM tumors. Different image enhancement methods have been used for decisive diagnosis in LM disease. The main purpose of using different image enhancement methods is to improve image and to display LM tumor more precisely. Because of this implementation, the radiologists have examined the improved MRI images more accurately. In addition to this, among the most effective results were obtained power-law transformation method and logarithmic transformation method. Therefore, the results obtained with LT method and PLT method were taken reference and tumor areas were compared with the results obtained with other image enhancement methods. The results obtained with different image enhancement methods applied to LM patients are shown in Figure 4.1.

The MRI images in Figure 4.1 belong to the same LM patients and also improved raw MRI images by LT method and PLT method are shown together. The best illustrations of tumor results are obtained with LT and PLT image enhancement methods. Tumors areas in MRI images were denoted by an arrow. Both radiologists determined tumors areas by separately with a consensus and the results obtained with other image enhancement methods were compared with the reference points which radiologists denoted by an arrow.

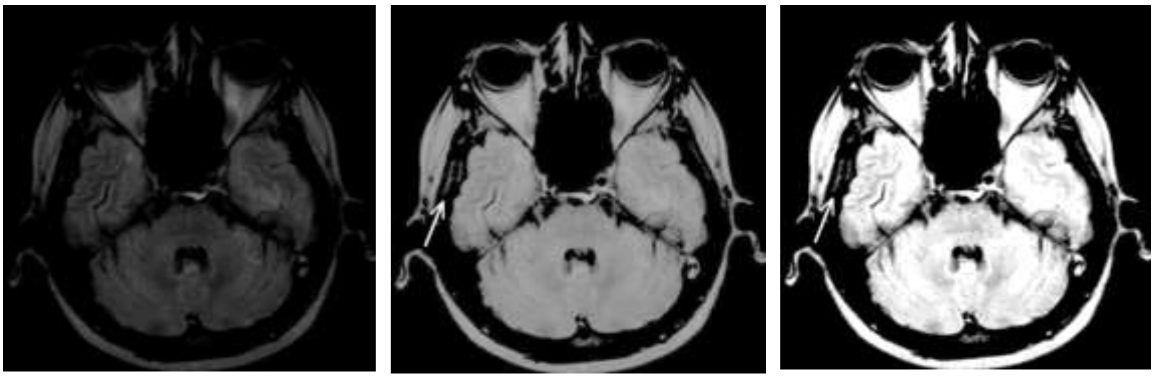

a) b) c)

Figure 4.1 Comparison of two different methods.
a) The Raw Flair MRI image, b) Improved Image by LT method,
c) Improved Image by PLT method

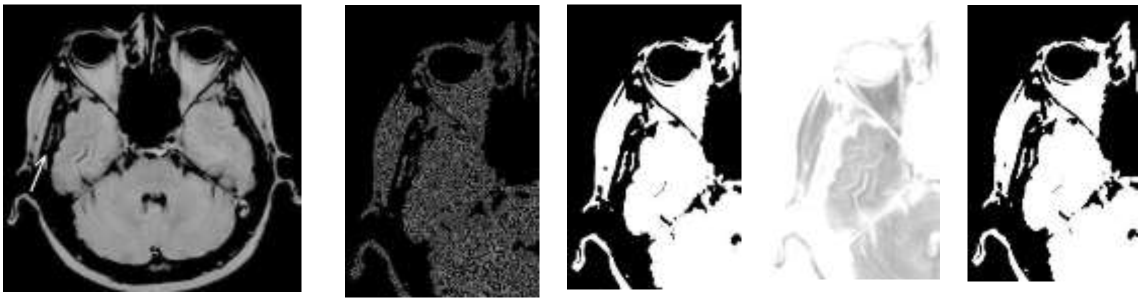

a) b) c) d) e)

Figure 4.2 Comparison of four different methods.
a) Represents improved image by LT method; b) represents improved image by BPS; c) represents improved image by GLS; d) represents improved by INT; e) represents improved image by thresholding method

In the Figure 4.2, some of results obtained by used the image improved methods were able to be similar. If Figure 4.2.a was taken reference, the results of Figure 4.2.b, 4.2.c and 4.2.e were similar except Figure 4.2.d.

Unfortunately, this success taken in some images has not been observed for other images. Images of some other patients in the study group are shown Figure 4.3.

Let's compare the results obtained with the other image enhancement methods according to the reference point marked with arrow. The tumor area in the Figure 4.4.a was determined by LT image enhancement method. When the marked point in the Figure 4.4.a is taken reference, it can be seen the partial success obtained in the Figures 4.4.b, 4.4.c and 4.4.e.

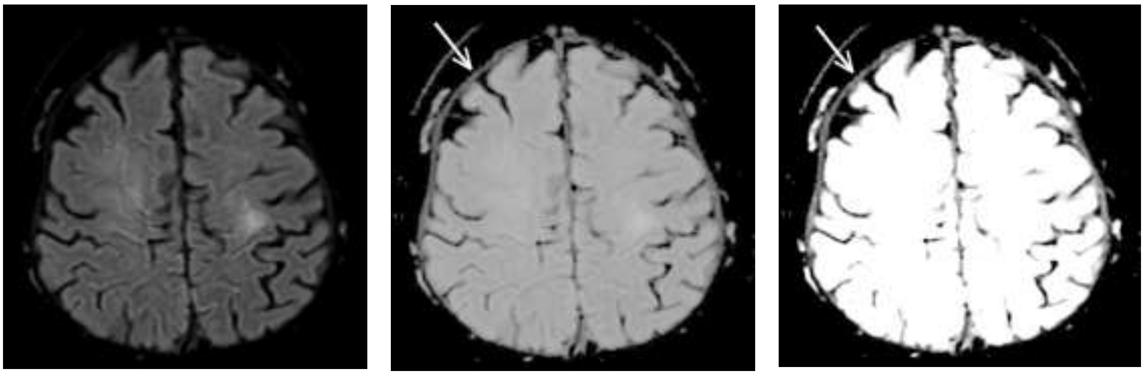

a) b) c)

Figure 4.3 Comparison of two different methods.
a) The Raw Flair MRI image, b) Improved Image by LT method, c) Image by PLT

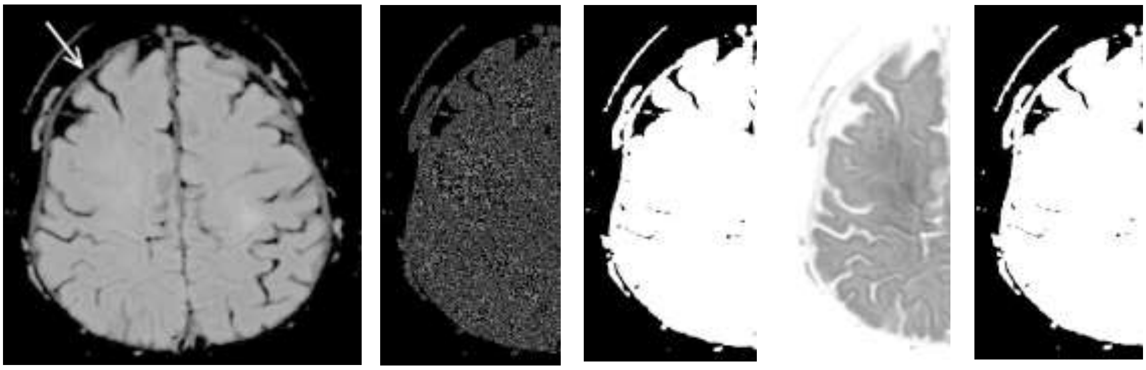

a) b) c) d) e)

Figure 4.4 Comparison of five different methods.
a) represents image by LT method; b) image by BPS; c) image by GLS; d) by INT; e) image by thresholding method

The tumor area in the Figure 4.4.d cannot be selected so easily compare to other results. The other parts of brain tissues are not displayed in the Figure 4.4.b, 4.4.c and 4.4.e and according to this, the awareness of the tumor areas cannot be compared with the results obtained with LT and PLT image enhancement methods. Because the tumor area in the Figure 4.4.b, 4.4.c, 4.4.d and 4.4.e can be realized with the reference Figure 4.4.a.

Let's evaluate on another image in study group Figure 4.5; let's compare the results obtained with the other image enhancement methods according to the reference point marked with arrow. Despite the reference above image obtained by the LT method, the tumor area cannot be selected clearly in the Figure 4.6.b, 4.6.c, 4.6.d and 4.6.e.

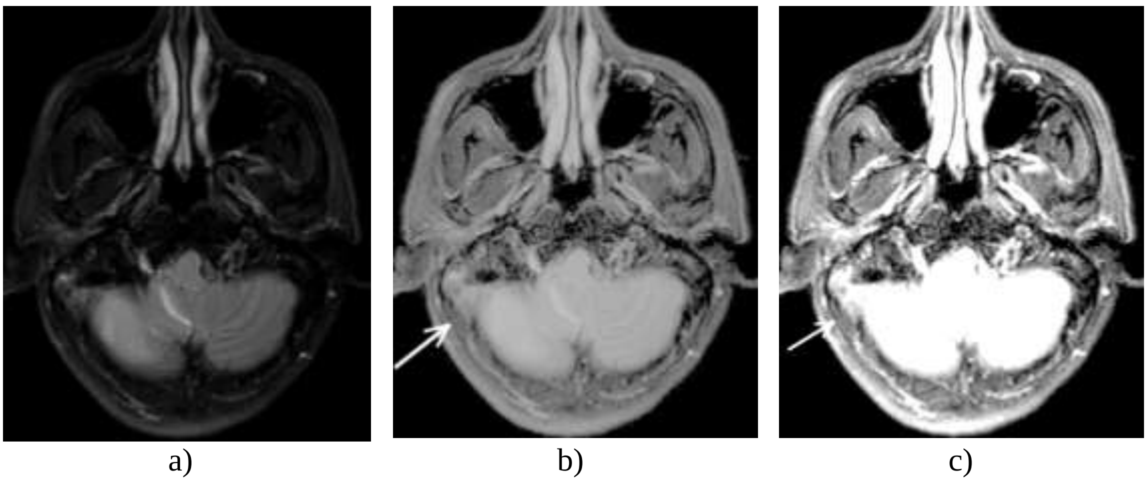

a) b) c)

Figure 4.5 Comparison of two different methods.
a) The Raw Flair MRI image, b) Improved Image by LT method, c) Improved Image by PLT

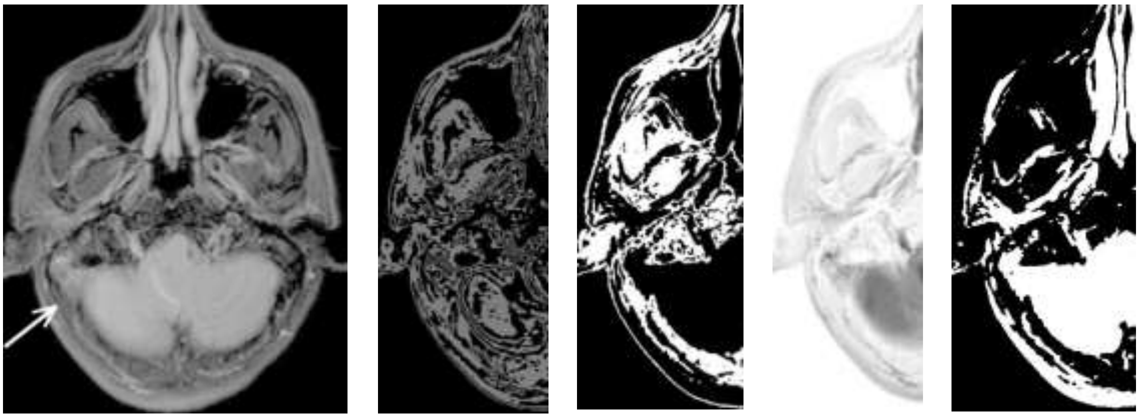

a) b) c) d) e)

Figure 4.6 Comparison of five different methods.
a) Represents image by LT method; b) represents image by BPS; c) represents image by GLS; d) represents by INT; e) represents image by thresholding method

Similar example situations have been observed in many MRI images of LM patients in the study group. There are three methods that obtained in the most effective results, these are logarithmic transformation, power-law transformation and contrast stretching methods. The results obtained with logarithmic transformation and power-law transformation are very similar through these three methods. The close results obtained with these two methods are statistically very high. On the other hands, the results obtained from contrast stretching method are statistically significant. The results of contrast stretching method are very low compared to the results obtained from logarithmic transformation and power-law transformation methods.

LM tumors emerge more clearly in the logarithmic transformation and power-law transformation methods. The observed significant difference can be used in the diagnosis process. It is very important consideration. The results obtained from contrast stretching methods are much better than raw MRI images and get more tangible improvement than raw MRI images. Although, the tumor areas revealed in contrast stretching method are marked out less than the other two methods.

Let’s evaluate the results images obtained with LT and PLT image enhancement methods. It could be diagnosed through 16 of 42 LM patients’ MRI images. There were 42 patients in the study group. It was diagnosed only in raw MRI images of 14 of 42 leukemia cancer patients (ALL cancer and AML cancer). After applying the LT and PLT image enhancement methods, the LM tumor areas were undiagnosed in only 2 of

14 leukemia cancer patients' MRI images (Table 4.1). Before image processing, the percentage rate of leukemia cancer is 28.6% of the raw images which are diagnosed by radiologists. On the other hand, after image processing methods, this ratio is 85.7% of images which are diagnosed by radiologists.

There were 12 patients in the study group who the first diagnosis with lung cancer. It was considered the raw MRI images of these 12 LM patients and only 3 patients were diagnosed to LM cancer in the first evaluation. The remaining 9 of 12 patients could not be diagnosed through raw MRI images. After LT and PLT image enhancement methods applied to diagnose LM cancer, the tumor areas were revealed in all patients' MRI images (Table 4.1). Before image processing, the percentage rate of lung cancer is 25% of the raw images which are diagnosed by radiologists. On the other hand, after image processing methods, this ratio is 75% of images which are diagnosed by radiologists.

There were 11 patients in the study group who the first diagnosis with breast cancer. It was considered the raw MRI images of 11 LM patients and only 8 patients were diagnosed to LM cancer in the first evaluation. After applying the LT and PLT image enhancement methods, the tumor areas were revealed in all patients' MRI images (Table 4.1). Before image processing, the percentage rate of breast cancer is 72.7% of the raw images which are diagnosed by radiologists. On the other hand, after image processing methods, this ratio is 27.3% of images which are diagnosed by radiologists.

There were 2 patients in the study group who the first diagnosis with gastric cancer. It was considered the raw MRI images of two LM patients and only one patient was diagnosed to LM cancer in the first evaluation. After applying the LT and PLT image enhancement methods, the tumor areas were revealed in both patients' MRI images (Table 4.1). Before image processing, the percentage rate of gastric cancer is 50% of the raw images which are diagnosed by radiologists. On the other hand, after image processing methods, this ratio is 100% of images which are diagnosed by radiologists.

There was one patient in the study group who the first diagnosis with renal cell cancer. It was considered the raw MRI images of one LM patient and it was not diagnosed to LM cancer in the first evaluation. After applying the LT and PLT image enhancement methods, the tumor areas were revealed in patient's MRI images (Table 4.1). Before image processing, the percentage rate of renal cell cancer is 0% of the raw images which are diagnosed by radiologists. On the other hand, after image processing methods, this ratio is 100% of images which are diagnosed by radiologists.

There was one patient in the study group who the first diagnosis with cervix cancer. It was considered the raw MRI images of one LM patient and it was not diagnosed to LM cancer in the first evaluation. After applying the LT and PLT image enhancement methods, the tumor areas were revealed in patient’s MRI images (Table 4.1). Before image processing, the percentage rate of cervix cancer is 0% of the raw images which are diagnosed by radiologists. On the other hand, after image processing methods, this ratio is 100% of images which are diagnosed by radiologists.

There was one patient in the study group who the first diagnosis with larynx cancer. It was considered the raw MRI images of one LM patient and it was not diagnosed to LM cancer in the first evaluation. After applying the LT and PLT image enhancement methods, the tumor areas were revealed in patient’s MRI images (Table 4.1). Before image processing, the percentage rate of larynx cancer is 0% of the raw images which are diagnosed by radiologists. On the other hand, after image processing methods, this ratio is 100% of images which are diagnosed by radiologists.

The results obtained from LT and PLT method with all the details are shown in the Table 4.1. Through 2 leukemia patients’ MRI images could not solely be diagnosed in 42 LM patients in the study group. All other 40 patients were diagnosed with MRI images obtained from image enhancement process. The success ratio is 95.2% and this ratio is actually high.

On the other hands, if it was looked at the results obtained from CS image enhancement process, the results were not so successful than the results obtained by LT and PLT image enhancement process.

For instance, 4 of 14 leukemia cancer could only be diagnosed to LM cancer with raw MRI images; after processing with CS image enhancement method, 5 of 14 leukemia cancer patients were only diagnosed to LM cancer Table 4.2. The remaining 9 patients of 14 leukemia cancer could not be diagnosed to LM cancer (Table 4.2).

Table 4.1 Results of image with LT and PLT methods

Cancer Types		Tumor before processing		Total	Tumor after processing		Total
		Exists	Non-Exists		Exists	Non-Exists	
ALL cancer	Number	4	8	12	11	1	12
	%	33.3%	66.7%	100%	91.7%	8.3%	100%
AML cancer	Number	0	2	2	1	1	2
	%	0%	100%	100%	50%	50%	100%
Lung cancer	Number	3	9	12	12	0	12
	%	25%	75%	100%	100%	0%	100%
Breast cancer	Number	8	3	11	11	0	11
	%	72.7%	27.3%	100%	100%	0%	100%
Gastric cancer	Number	1	1	2	2	0	2
	%	50%	50%	100%	100%	0%	100
Renal Cell cancer	Number	0	1	1	1	0	1
	%	0%	100%	100%	100%	0%	100
Cervix cancer	Number	0	1	1	1	0	1
	%	0%	100%	100%	100%	0%	100%
Larynx cancer	Number	0	1	1	1	0	1
	%	0%	100%	100%	100%	0%	100
Total of all patients	Number	16	26		40	2	
	%	38.1%	61.9%		95.2%	4.8%	

Before image processing, the percentage rate of leukemia cancer is 28.6% of the raw images which are diagnosed by radiologists. On the other hand, after image processing methods, this ratio is 35.7% of images which are diagnosed by radiologists.

3 of 12 lung cancer could only be diagnosed to LM cancer with raw MRI images. 6 of 12 lung cancer could only be diagnosed to LM cancer with CS image enhancement method. The remaining 6 patients of 12 cancers could not be diagnosed to LM cancer (Table 4.2). Before image processing, the percentage rate of lung cancer is 25% of the raw images which are diagnosed by radiologists. On the other hand, after image processing methods, this ratio is 50% of images which are diagnosed by radiologists.

8 of 11 breast cancer could only be diagnosed to LM cancer with raw MRI images. Any unsuccessful results were obtained despite applying CS image enhancement method (Table 4.2). Before image processing, the percentage rate of breast cancer is 72.7% of the raw images which are diagnosed by radiologists. On the other hand, after image processing methods, this ratio is not changed.

One of two gastric cancers could only be diagnosed to LM cancer with raw MRI images. After applying CS image enhancement method, it was diagnosed to LM cancer with MRI images of two gastric cancer patients. Before image processing, the percentage rate of gastric cancer is 50% of the raw images which are diagnosed by radiologists. On the other hand, after image processing methods, this ratio is 100% of images which are diagnosed by radiologists (Table 4.2).

There were only one recal cell cancer, one cervix cancer and one larynx cancer patient in the study group. When the first MRI images of all three patients were examined, they could not be diagnosed through raw MRI images. As a result of improvements with CS method was not changed (Table 4.2). Before image processing, the percentage rate of renal cell cancer is 0% of the raw images which are diagnosed by radiologists. On the other hand, after image processing methods, this ratio is not changed. LM tumor could not be revealed after processing of CS method.

When the total of all patients are considered, the results are 22 of 42 patients. It means that the tumor areas are revealed in 22 patients' MRI images, the tumor areas cannot be revealed in the other 20 patients' MRI images.

Table 4.2 Results of image with CS method

Cancer Types		Tumor before processing		Total	Tumor after processing		Total
		Exists	Non-Exists		Exists	Non-Exists	
ALL cancer	Number	4	8	12	5	7	12
	%	33.3%	66.7%	100%	41.7%	58.3%	100%
AML cancer	Number	0	2	2	0	2	2
	%	0%	100%	100%	0%	100%	100%
Lung cancer	Number	3	9	12	6	6	12
	%	25%	75%	100%	50%	50%	100%
Breast cancer	Number	8	3	11	8	3	11
	%	72.7%	27.3%	100%	72.7%	27.3%	100%
Gastric cancer	Number	1	1	2	2	0	2
	%	50%	50%	100%	100%	0%	100
Renal Cell cancer	Number	0	1	1	0	1	1
	%	0%	100%	100%	0%	100%	100
Cervix cancer	Number	0	1	1	0	1	1
	%	0%	100%	100%	0%	100%	100%
Larynx cancer	Number	0	1	1	0	1	1
	%	0%	100%	100%	0%	100%	100
Total of all patients	Number	16	26		22	20	
	%	38.1%	61.9%		52.4%	47.6%	

When radiologists evaluate the raw MRI images, the percentage is 38.1%, that is, the tumor areas are revealed in nearly four-tenth patients' MRI images, however when MRI images are , the percentage is 61.9% and it is higher than 50%, it is a bit successful but when this result is compared with the result obtained by LT and PLT methods, it is not as successful as the first the results obtained by LT and PLT methods.

Although CS image enhancement method improves the MRI image qualities, the results were not as good as the results obtained from LT and PLT methods. The results are shown in the Table 4.2 in details. The statistically significant results are demonstrated in Table 4.8 between LT and PLT image enhancement methods and CS image enhancement method. The sensitivity results of high degree ratio were obtained from LT and PLT methods. On the other hand, the successful results were obtained from CS method.

In the Table 4.3, the total number of patients groups, data of mean age of these located in study group and the percentage of these are given in detail. The mean age of 12 ALL leukemia patients was approximately 18.18 and the mean age of 2 AML leukemia patients was approximately 49.46. There were 12 lung cancers and their mean age was approximately 57.73. The mean age of third group, breast cancer patients, was approximately 38.5. There were 2 patients who were clinically diagnosed with gastric cancer and their mean age was 57. The mean age of renal cell cancer patients was 74. The mean age of cervix cancer patient was 72 and the mean age of larynx cancer patient was 38.

Table 4.3 The first clinical diagnosis of patients and mean age of patients groups by details (* leukemia cancer)

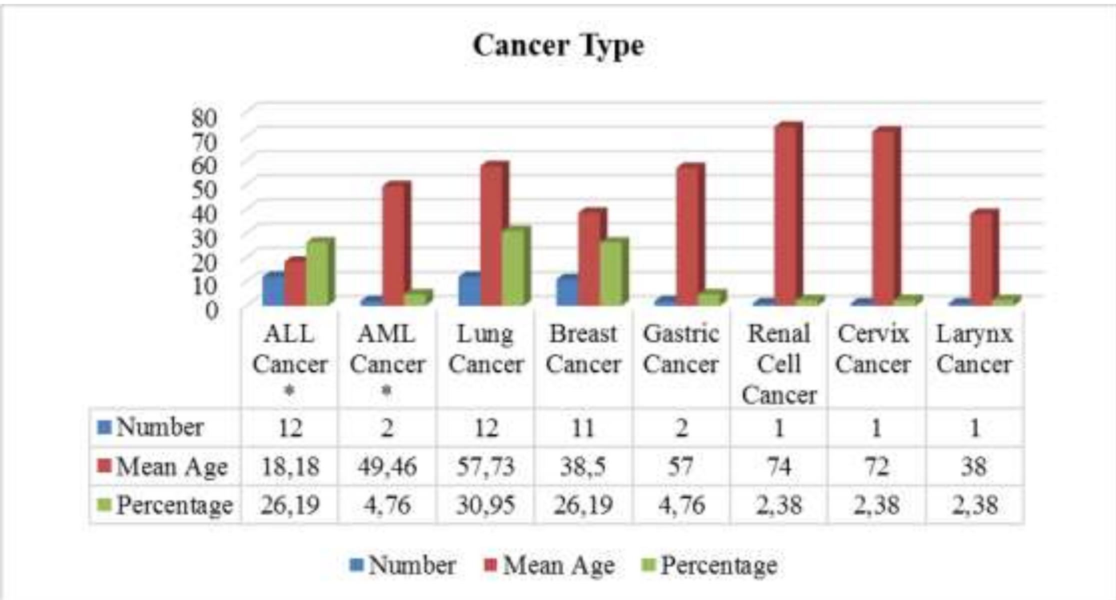

Contrast- MRI images are used for radiologists or physicians who use for commenting through MRI images to diagnose the disease. The medicine is injected to get contrast- images from patients such as Gadolinium (Gd). The contrast- image gives significant results compared to Flair image in each time. This is because the medicine is injected into the patient for involvement on tissue.

Despite the more successful results obtained in contrast- image than the results of Flair image, the desired evaluation cannot always be expected these both images. MRI images contain rich information; however some information is stored in the dark areas. For instance, despite acquisition of the LM tumor areas on the MRI images, these areas cannot be realized through MRI images. Tumor areas may not be displayed even in the contrast- MRI images. Contrast- MRI image and Flair image of the same LM patient are shown in the following Figure 4.7. The resulting more detailed contrast- images were examined, approximately 4 patients were diagnosed as metastases.

The obtained images are contained very rich information. LT method and PLT method are revised that reveal the hidden information in the image. In our study, it is used to elicit both leptomeningeal surface and LM tumors in the MRI brain images with LT image enhancement method. When LT method and PLT method are applied to brain MRI images, in the first stage leptomeningeal surface is intended to distinguish.

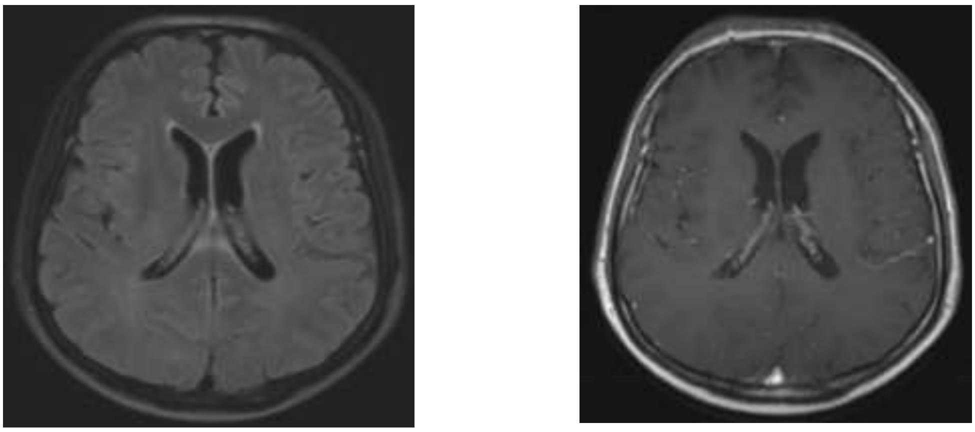

a) b)

Figure 4.7 Differences of the same patient's the FLAIR MRI image and contrast- MRI image. a) The different appearances of FLAIR, b) Contrast- MRI images

After distinguishing the leptomeningeal surface on MRI images, the presence of tumors areas through leptomeningeal surface is fastened down in the second step. LT and PLT image enhancement methods are performed on the image to detect the tumors which is proved to be in macroscopic or microscopic sizes in autopsy results. Before being applied the image enhancement methods, the tumor areas were detected in sixteen of 42 patients' raw MRI images to diagnose LM cancer. After application of the LT and PLT image enhancement methods, the tumor areas have observed in 40 of 42 patients' MRI images.

Image enhancement methods are used in many different areas. Especially, many successful results continue to be obtained in the medical field. When new images obtained are analyzed, the success is remarkable by LT method, PLT method and CS method. Positive results were obtained not only in contrast- MRI images but also in flair MRI images by these methods. Sharper image is obtained in contrast- MRI images compared with flair MRI images; the tissues in contrast- MRI images are more selective state. Because the drug is injected into the patient to get contrast- MRI images and more detailed images are obtained with injected drugs through tissue.

When CSF fluid analysis was examined to suspect consistent with positive or positive in MRI images of research group, there had not been reported to observe any metastases. In other words, each time tumor tissue may not be observed in the unprocessed MRI images. This situation, diagnosis of advanced level cancer especially as leptomeningeal metastases disease is a major problem.

When LT method, PLT method and CS method are applied the obtained brain MRI images of LM cancer patients, leptomeningeal layer has clearly revealed. The main purpose of our study is that contaminated tumor cells or tissues on leptomeningeal surface are revealed. The purpose is that the request information on rich MRI images is simplify, in other words, distinguish contaminated cancer cells from surrounding tissues.

For this purpose, the different image enhancements methods have been applied to the MRI images to distinguish the LM tumors. The more successful results were obtained to distinguish LM tumors from LT, PLT and CS image enhancement methods than other methods. Both Flair and contrast- MRI images are significantly distinguished leptomeningeal surface by three methods.

The results of 1.5 tesla standard MRI imaging system used to determine a diagnosis of LM cancer consists of some problems. These encountered problems in diagnosis of the disease are the biggest obstacle. Early diagnosis often helps to start early treatment, therewithal; early treatment usually heals the patient and steps into a new life. Early diagnosis is vital importance for an advanced type of LM cancer. Patients already try to cope with a cancer such as breast cancer, tumors in the body causing a second cancer by gaining various sizes or obtaining within CSF fluid is a very big problem for the patient.

Morale is the biggest weapon to beat cancer disease for patients. During cancer patients struggle with the cancer disease, the second phase of the cancer disease gives a very negative impact on the patient's psychology. The early diagnosis is vital importance in both improvement the quality of the life and prolongation of the life.

In our study, it is aimed to come in sight the details of in dark region with improving image quality and determine early unobserved phenomenon in diagnosis with applied image processing method. It is the first literature in this field to obtain supporting data in our study. We hope that this study will support with more cancer events.

The obtained results of the second study was performs as follows. CSF examination evaluated in the pathology unit carries a certain value for all diseases intended to diagnose the disease such as leptomeningeal metastases. The second study has been prepared with reference of exact results of the CSF examination. The main aim of this study is to compare between the raw MRI images results and the MRI images results according to exact CSF examination results.

The patient suspected leptomeningeal metastases by cytopathological evaluation in pathology department has been focused, the patient who diagnosed to positive, doubtful and negative taken from pathology archives and these cases have been re-evaluated by a particular pathologist to get confirmation of diagnosis. MRI images of the same patients which were generated picture at the same time were re-examined by a particular radiologist and they were confirmed. The confirmation of all patients are given in Table 4.4.

CSF examination results and raw MRI results are compared and the comparison results between these are in the following. Positive results were given 18 patients by CSF examination. When the raw MRI images of the same 18 patients were examined, positive results were given only 7 patients. The rate of this results is 50%. Despite of 7 positive results, 11 patients' results were given negative according to raw MRI examinations.

11 patients' CSF results are positive and but the raw MRI results are negative the rate is 47.8%. According to other CSF results, 8 patients' results are negative and 4 patients' results are doubtful and respectively the rates are 34.8% and 17.4%.

4 patients' raw MRI results are positive but CSF results are negative and the rate is 28.6. 7 patients' raw MRI results are positive and also CSF results are positive and finally 3 patients' raw MRI results are positive but CSF results are doubtful. The rates are respectively 28.6% and 50% and 21.4%.

Table 4.4 Comparison of Raw MRI * CSF Pathology Cross Tabulation

			CSF Pathology			Total
			N*	P**	D***	
Raw MRI	N*	Count	8	11	4	23
		% within MRI	34,8%	47,8%	17,4%	100,0%
		% within CSF	66,7%	61,1%	57,1%	62,2%
	P**	Count	4	7	3	14
		% within MRI	28,6%	50,0%	21,4%	100,0%
		% within CSF	33,3%	38,9%	42,9%	37,8%
Total		Count	12	18	7	37
		% within MRI	32,4%	48,6%	18,9%	100,0%
		% within CSF	100,0%	100,0%	100,0%	100,0%

N*: negative; P**: positive; D***: doubtful

The comparison results between images by image enhancement methods and the exact reference CSF examination results are as follows. 18 patients were diagnosed to LM cancer based on CSF examination results. When images were re-examined, all of 18 patients' results which diagnosed to positive according to CSF examination were positive.

4 patients' MRI results are negative and also CSF results are negative and the rate is 66.7%. One patient MRI result is negative however CSF result is positive and the rate is 16.7%. One patient MRI result is negative but CSF result is doubtful and the rate is 16.7

Table 4.5 Comparison of MRI * CSF examination cross tabulation

			CSF examination			Total
			N*	P**	D***	
MRI	N*	Count	4	1	1	6
		% within MRI	66,7%	16,7%	16,7%	100,0%
		% within CSF	33,3%	5,6%	14,3%	16,2%
	P**	Count	7	17	4	28
		% within MRI	25,0%	60,7%	14,3%	100,0%
		% within CSF	58,3%	94,4%	57,1%	75,7%
	D***	Count	1	0	2	3
		% within MRI	33,3%	,0%	66,7%	100,0%
		% within CSF	8,3%	,0%	28,6%	9,1%
Total		Count	12	18	7	37
		% within MRI	32,4%	48,6%	18,9%	100,0%
		% within CSF	100,0 %	100,0%	100,0%	100,0%

N: negative; P: positive; D: doubtful

7 patients' MRI results are positive but CSF results are negative and the rate is 25%. 17 patients' MRI results are positive and also CSF results are positive and the rate is 60.7%. 4 patients' MRI results are positive but CSF results are doubtful and the rate is 14.3%. One patient MRI result is doubtful but CSF result is negative and the rate is 33.3%. 2 patients' MRI results are doubtful and also CSF results are doubtful and the rate is 66.7%.

The comparison results between images by image enhancement methods and the exact reference CSF examination results are as follows. 18 patients were diagnosed to LM cancer based on CSF examination results. When images were re-examined, all of 17 patients' results which diagnosed to positive according to CSF examination were positive.

These results show that the MRI images by image enhancement methods give especially better results than raw MRI images based on the exact CSF examination results and especially indicate a more precise and sensitive method for the detection of positive cases which are diagnosed with the CSF examination. Because the MRI image results are closer to the exact cytopathology results and thus the MRI images give valuable results.

The sensitivity of this study is 79.31%, specificity is 68.89% and prevalence is 39.19%. In addition to this, the positive predictive 62.16% and negative predictive is 83.78%. According to this results, the sensitivity and specificity results are high and valuable.

These results show us, when the image enhancement methods are applied to MRI images, the results can be sometimes better than pathology results. However, if the number of subjects are increased, more precise results can be obtained.

Table 4.6 Comparison of MRI images according to CSF examination results

	CSF examination	The Raw image	The image
Positive	18	14	28
Negative	12	23	6
Doubtful	7		3

Some of CSF examination results were obtained negative, despite of positive MRI image results. The results are concluded according to this regarding results:

- The tumor involvement on the leptomeningeal layer may not spill into CSF fluid. In this case, despite of dissemination on leptomeningeal layer, insufficient amounts of tumors spill over CSF fluid, it may not be a positive result for the examination.

- The CSF examination results of the same patient obtained in periodically can be different with each other, because the disease can be diagnosed in the later CSF examination except for the first sample.
- If the patient diagnosed positive confirmation with MRI images despite of negative confirmation concluded on CSF examination, it is really available leptomeningeal metastases disease. The clarification of the situation can state with certainty to obtain further evaluation or obtain biopsy results.

As a result, the findings from this study, we think that evaluation of together with the cytopathology results and the enhancement MRI results is more valuable than evaluation of together with the cytopathology results and the raw MRI results.

CONCLUSION

CNS is a unique structure that process myriad information and these information in the resting phase transfers peripheral nervous system. CNS consists of two buildings including the brain and the spinal cord. On the other hand, PNS consists of all other neural structure radiating from the spinal cord to the rest of the body [21]. Meninges layers are just below the skull surrounding the brain. This layer wraps the brain and as well as helps to balance the brain in the skull.

Meninges layer consists of three sub-layers, respectively these layers from outside to inside be Dura mater layer, Arachnoid mater layer and Pia mater layer. Meninges layer is inside the skull as well as surrounds the brain and spinal cord tightly [22]. The top layer of this structure (Dura mater layer) is very rigid structure and adhered to the skull, the middle layer of this structure (Arachnoid mater layer) is like spider structure and possesses the blood vessels that supply the brain oxygen and energy and the blood vessels are reached through the brain in the innermost layer enveloping layer of brain. Pia mater and Arachnoid mater layer is taken as leptomeningeal layer together.

The blood flow to the brain is provided in leptomeningeal layer and malignant tumors reach brain in this layer. The spreading of the cancer tissues in this layer is called leptomeningeal metastases. LM disease usually emerges in advanced situations of lung cancer, renal cell cancer, melanoma, colorectal carcinoma and some prostate cancer [37, 77]. Malignant tumor cells spread in different ways to the leptomeningeal layer and subarachnoid layer. The propagation occurs by hematogenous spread from choroid plexus veins or arachnoid veins, direct spread from parenchymal or along the way of perineural in cranial nerve. Malignant tumor cells spread with blood or cerebrospinal fluid in spinal fluid [27 – 29].

Some symptoms of the disease in patients with leptomeningeal metastases are seen that headache, local weakness, focal weakness, altered mental status, seizures and ataxia [39, 75]. In the case of cancer patients of %67 contacted with complaints mentioned above can be brain metastases [76]. Leptomeningeal metastases cancer disease is one of the most difficult to diagnose and early diagnosis of leptomeningeal metastases is taken an important place for the treatment of disease. Early diagnosis prolongs the life of patient as well as improves the quality of life. Spreading of malignant tumor cells in CSF fluid is very risky to cut through this type of cancer through medical operation.

Imaging system and CSF fluid analysis are used for diagnosis of disease. Imaging system is the first referred choice. There are many imaging system are used for diagnosis, however such system as CT and MRI are the first choices. MRI imaging system helps enable viewing of soft tissues more comforTable compared to CT imaging system. Images obtained from MRI imaging system contain very rich information. However, these information may not always easy to read. radiologist may not easy to read the images of containing malignant tumors contaminated in CSF fluid layer such disease as LM cancer on MRI images. This situation is a serious obstacle to the diagnosis.

Early detection is vital, especially for patients with cancer patients. Image enhancement applications are one of the methods used for early diagnosis. Many image enhancement methods are in the question used for the different purposes in different areas. Logarithmic transformation is basic tools for dynamic range manipulation. Hidden details in MRI images can be revealed through this method.

Early diagnosis is a very important step and the results obtained from images were observed by the radiologists. The successful results are taken with logarithmic transformation method whether in flair MRI images or contrast- MRI images. Obtaining the successful results are very important for starting the early treatment based on a report prepared by radiologists by oncologists.

The enhancement through MRI images was done with LT and PLT methods and only a certain range of the pixel were compressed and the others were expanded. Thus, the extremely high probability success was obtained from values. The diagnosis of LM disease through MRI images was performed with CS image enhancement method. The values of specificity and sensitivity probabilities are given in the following Table 4.7 and Table 4.8.

The obtained statistically highly successful results were evaluated by two radiologists, a biostatistics doctor and an oncologist doctor who were contributed to the thesis.

Table 4.7 The Table of Sensitivity, Specificity, Positive Predictive and Negative Predictive according to LT and PLT methods

	Disease	Non-Disease	Total
Positive	16	26	42
Negative	40	2	42
	56	28	84

The sensitivity result is 92.85%, the specificity result is 71.42% and the prevalence result is 33.33%. In addition to this, positive predictive result is 61.9% and negative predictive is 95.23%. According to these results obtained from Table 4.7, the sensitivity and the specificity results of this study is very high.

When the results obtained from CS method are analyzed, the sensitivity result is 56.52%, the specificity result is 57.89%, the prevalence result is 54.76% and the positive predictive result is 61.9%, the negative predictive result is 52.38%. According to these results obtained from Table 8, the sensitivity and the specificity results are high but these are not as good as the results obtained from LT and PLT methods in Table 4.7.

On the other hand, the results of LT and PLT methods were analyzed with SPSS software. The likelihood ratio of the results, p = 0,000000005 (P < 0,001), were obtained by applying the chi-square tests. The statistical results are highly successful results. The hidden details through images are highlighted with LT and PLT image enhancement methods. When we analyze these two different methods, the first method is not suitable for this study. Because all statistical methods cannot be applied to all different studies (Table 4.9). The results of all three methods are illustrated in the Table 4.9.

Table 4.8 The Table of Sensitivity, Specificity, Positive Predictive and Negative Predictive according to CS method

	Disease	Non-Disease	Total
Positive	16	26	42
Negative	22	20	42
	38	46	84

Table 4.9 The statistical results of LT method, PLT method and CS method and comparison of results of obtained by three methods

	Diagnosis of LM disease with LT and PLT methods		Diagnosis of LM disease with CS method		Comparison of three methods
Numbers of patients	Defined	Non-defined	Defined	Non-defined	0.000 (< 0.001)
	40	2	22	20	
p-value	0.000 (< 0.001)		0.031 (< 0.05)		

The result of CS method was analyzed with SPSS software. The likelihood ratio of the result, p = 0.031 (P < 0.05), was obtained by applying the chi-square tests. The obtained result was statistically significant. The result of this ratio has been shown that the CS method can be used to diagnose LM disease. In addition to this, the successful results have been obtained compared to the diagnosis over the raw image (Table 4.9).

The interesting details are in the Table above. The extremely successful statistical results have been obtained with LT and PLT image enhancement methods. The results obtained from the CS method have been successful compared to the results of raw MRI images. Despite the successful results of CS method, this extremely low result cannot be compared to the results obtained from LT and PLT methods for the diagnosis of LM disease.

When raw MRI images of 42 patients in the study group have been examined, it is shown that the 35 patients' leptomeningeal surface could be detected. Whether the images are the raw contrast- brain MRI images or the raw Flair MRI images, the leptomeningeal surface cannot always be displayed. The leptomeningeal surface of all patients has been realized in MRI images and the significant differences have been obtained. MRI images contain very rich information as mentioned earlier, however all information does not display through MRI images. The simplest example is to display leptomeningeal surface.

6 of 12 ALL cancer patients were not performed the CSF examination. A patient's CSF examination result was positive, 3 of these patients' results were evaluated negative and however, the other 2 patients' results in the group were evaluated and the undefined results were obtained.

Table 4.10 The noticeable numbers of leptomeningeal surface through MRI images

	Before image enhancement process	After image enhancement process
The noticeable leptomeningeal surface number through MRI images	35	42
The unnoticeable leptomeningeal surface number through MRI images	7	0

Eight of 12 lung cancer patients were not performed the CSF examination. A patient's CSF examination result was evaluated suspicious, a patient's result was evaluated positive and 2 patients' results were evaluated negative.

The cancer patients in the study group were ranked according to types of cancer. The CSF examination results are sequenced by each type of cancer group. The CSF examination result of one AML cancer patient was evaluated positive and other patient's CSF examination result was not evaluated because of insufficient CSF flood materials. The CSF examination of larynx cancer patient was undone. The CSF examination of renal cell cancer patient was not evaluated because of insufficient CSF flood materials.

Table 4.11 The CSF examination results according to cancer types

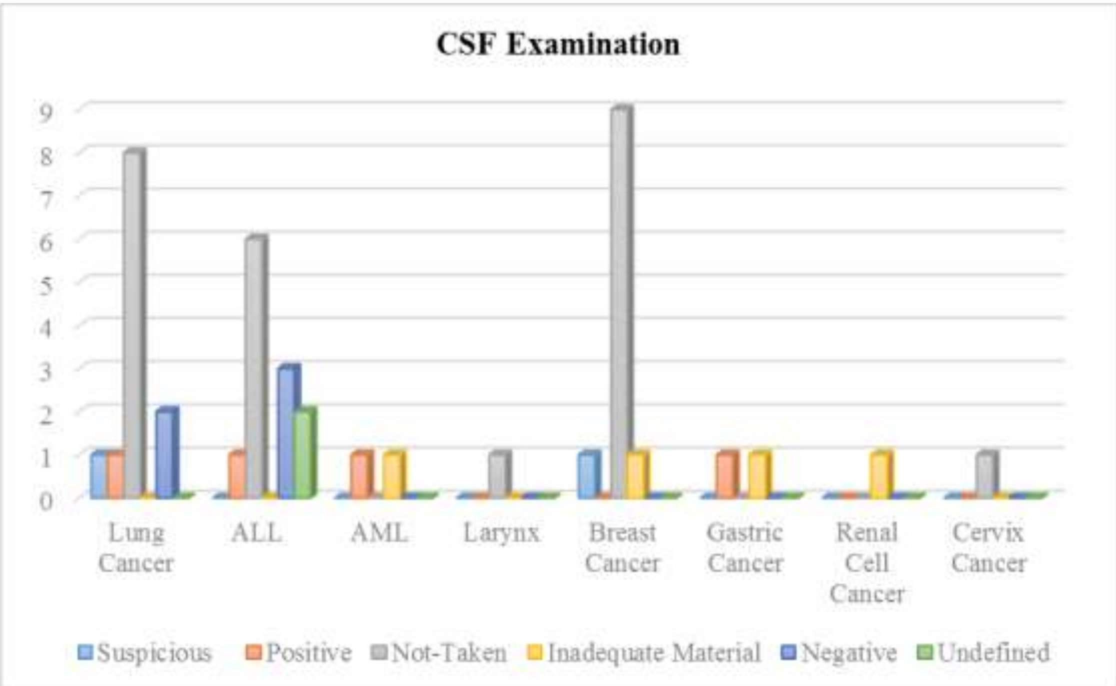

The CSF examination of cervix cancer was not performed because of untaken CSF flood materials. The CSF examination of only 2 of 11 breast cancer was performed in the study group. 1 of 2 patients result was suspicious and other CSF examination failed because of taking not enough liquid of CSF fluid. The analysis of CSF examination was not done for the remaining nine patients.

1 of 2 gastric cancer patient's result was made positive diagnosis and other patient result was not investigated because of taking inadequate CSF fluid material.

If we examine the Table 4.11, the results of CSF examination of 16 LM cancer patients do not match. Meanwhile, 16 patients were diagnosed to LM cancer through the raw MRI images. The raw MRI examinations of 2 patients were diagnosed to LM cancer, on the hand, their CSF examination results were suspicious. None of these 16 patients' CSF examination results were positive. 9 of 16 patients' CSF examination were not taken. 2 patients' CSF examinations were not done properly because of taking inadequate material. 2 patients' CSF examinations were negative and finally the rest of a patient's CSF examination result was uncertain.

The results of 26 patients' CSF examinations were also different from each other. These patients in the study group diagnosed LM cancer and did not diagnose through raw MRI images examinations.

Table 4.12 The results obtained with raw MRI images examination and the results of CSF examination were given together

		CSF Fluid Examination					
		S*	P*	NT*	IM*	N*	U*
MRI Results	Positive	2	0	9	2	2	1
	Negative	0	2	16	2	3	1

S=suspicious; P=positive; NT=not-taken; IM= inadequate material; N=negative; U=undifined

The CSF examination results of 4 patients were positive. 16 of 26 patients' CSF examinations were not taken. 2 of 26 patients' CSF examination were not done properly because of taking inadequate material. 3 patients' results were negative and finally the rest of a patient's CSF examination result was uncertain. The result of CSF examination process is more accurate compared to the results obtained from MRI images. In some cases, CSF examination may not achieve the desired results (Table 4.12).

DISCUSSIONS

There are 42 patients in the study group. The majority of patients admitted to Dicle University hospital oncology department and the remaining parts of patients admitted to Diyarbakır Gazi Yaşargil Education and Research hospital oncology department. Patients who caught LM disease and admitted to the oncology department were selected. There were no preliminary criteria for patients. Patients in different gender and different range of age were available. Data of the patients belong between 2003 and 2013.

The first diagnosis given to the patient was different from each other. Clinically the initial diagnosis of patients was different such as lung cancer, leukaemia and etc. before turning into LM disease. MRI and CT imaging systems and CSF examination are used to diagnose the LM disease. Results of CSF examination obtained in the majority of patients are more precise in diagnosis of LM disease than results provided imaging systems. Results obtained with CSF examination which helps the diagnosis of the LM disease are acquired later than results obtained by MRI and CT imaging systems. The data of the first diagnosis of 42 patients in the study group and the percentages of patients in the group are shown in Table 4.13.

Table 4.13 Clinical data of patients in research group

Clinically Initial Diagnosis	Number	Percentage
ALL Cancer*	12	28.57 %
AML Cancer*	2	4.76 %
Lung Cancer	12	28.57 %
Breast Cancer	11	26.19 %
Gastric Cancer	2	4.76 %
Renal Cell Cancer	1	2.38 %
Cervix Cancer	1	2.38 %
Larynx Cancer	1	2.38 %
Total	42	100%

There were 12 acute lymphoblastic leukaemia (ALL) and 2 acute myeloid leukaemia (AML) cancer patients in study group. Leukaemia cancer patients constituted 33.33 % of the total study group. The number of lung cancer patients was 12 and constituted approximately 28.57 % of the group. The numbers of breast cancer patients who they were the third weight in the study group were 11 and constituted approximately 26.19 % in the group. There were 2 LM cancer patients who the first clinical diagnosed with gastric cancer. They constituted approximately 4.76 % in group. There were 3 patients who the first clinical diagnosis of renal cell cancer, cervix cancer and larynx cancer patients. Each of patients constituted approximately 2.38 % in the study group.

The first clinical diagnosis of the patient and the mean age of the patients groups are given in detail in the Table 4.14.

The mean age of 42 patients was 43.67 (± 19.43), 18 of these patients were male and 24 patients were female. The mean age of male was 44.11 (± 18.47) and the mean age of female was 43.33 (± 20.51) (Table 4.14).

Soft tissue images are received successfully with MRI imaging system compared to other imaging systems. Especially, imaging of brain tissue with MRI imaging system gives more successful results compared to such imaging system as CT imaging system [48, 78 – 81]. The reason for this is that MRI imaging system is used the magnetic field. This event occurs as a result of exposure of the atoms in the individual’s soft tissue in the magnetic field. The MRI machine allows the movement of the atoms in the soft tissue with creating strong magnetic field, that is, magnetic field strength up to about 30,000 times gravity. MRI machine benefits from the instant displacement of the atoms which is located in soft tissues and moved freely.

Table 4.14 Demographic data Table of patients

	Number (%)	Mean age ± standard deviation
Male	18 (42.9)	44.11 (± 18.471)
Female	24 (57.1)	43.33 (± 20.506)
Sum	42 (100)	43.67 (± 19.429)

Thus, image sections are received with thanks atoms moving within the tissue. The movement of the atoms in the hard tissue such as bone is much harder than soft tissue such as brain tissue. The atoms in the soft tissue moves easier. MRI device is obtaining the desired cross-section images with instant changes of H^+ (hydrogen positive) atoms located in the soft tissues.

The process of imaging of the brain tumors with MRI imaging systems is received earlier than CSF examination results. Time differences are important not to be ignored in case of emergency situations or in pre-treatment for the purpose of early diagnosis. This is due to the delay and urgency of the situations, nearly all patients will be asked for MRI images at first.

The results obtained from the CSF examination are more precise than the results obtained from the MRI imaging system. Biomarkers are examined in CSF fluid and the more precise results are obtained from the examination. Studied biomarker gives more precise data whether LM disease exists or not because of that CSF examination is more preferred than MRI examinations.

Received MRI images of 42 patients who suspected with LM disease were examined at different dates. MRI images which were examined separately in different dates were taken from Dicle university hospital radiology unit. There was an ethics committee report on the acquired images. When MRI images were assessed, only 18 patients were diagnosed with LM disease.

Although patients' first clinical diagnosis is different, LM disease is more important compared to other cancer types, because progression of cancer such as lung cancer is advanced to cause dissemination of another type of cancer such as LM cancer. The diagnosis of LM disease is, therefore, more difficult than other cancer types. LM disease tumors may be in size of either macroscopic or microscopic size in CSF fluid.

There are all sequences of the MRI images of patients in the study group and are also contrast- images (used MRI sequences; T1 axial, coronal, sagittal, T2 axial, coronal, Flair axial, sagittal and contrast- T1 axial, coronal and sagittal images). The missing MRI images or blur MRI images as a result of patient motion when image retrieving process are not evaluated. The used MRI machine has 1.5 tesla properties.

T1 and T2-weighted images were analyzed by radiologists in the study. Oncology doctors asked the CSF examination in order to obtain more precise results. The images which the brain tissue was less displayed or not at all sequences were removed in evaluation process such as mouth, skull, jawbone and etc. Tumors of the LM disease were not displayed in the MRI images obtained in these regions.

It was aimed to obtain better results in the evaluation phase of MRI images for some prominent disease such as LM disease in this study. In addition to this, it was also aimed to increase the sensitivity of MRI images system, especially for LM disease due to the significant differences between the obtained results. Extensive research was made to increase sensitivity of MRI imaging system. The studies were generally to increase the strength of the MRI imaging system. It was aimed to increase the tesla force of MRI imaging system for increment of the visibility of the tumors areas on the soft tissue or changes were made on the amount of drug used to obtain contrast- MRI images.

Substance called gadolinium is injected to patient in order to obtain the standard contrast- MRI images. The purpose of this process is that the tissue uptake of the substance injected. Visibility of details on tissue is increased when more involvement occurs and MRI images are more pronounced. LM tumors in the CSF fluid are tried to notice on MRI images of the patients with injected gadolinium material to the patient.

Contrast- MRI images obtained with gadolinium (Gd-MRI) have concluded that do not enough detail in some studies. For instance, the visibility of LM tumors proportion on Gd-MRI images is 66% [82]. The studies are carried out overcome this situation and to increase the sensitivity of images such as the amount of magnetization saturation injected using combination of all sequences of MRI images and etc. [79].

In the Figure 4.8, it is illustrated two different MRI images belongs to two different patients. LM tumors cannot be detected in both raw Flair MRI image and contrast- MRI image. These two patients were diagnosed with LM disease. Furthermore, if adequate enhancement process is done on MRI images, the awareness of LM tumor will be increased.

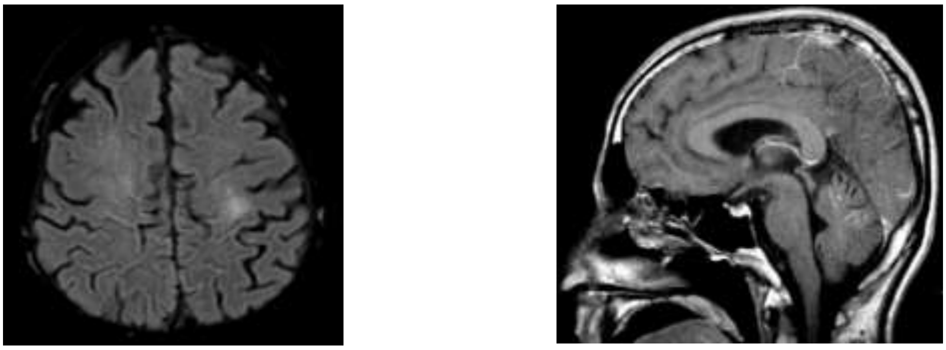

a) b)

Figure 4.8 Differences of the FLAIR MRI image and contrast- MRI image. a) LM patient's Flair image, b) contrast- MRI image

The visibility of LM tumors on MRI images is so low in spite of injecting the Gd substance (nearly 66%), the visibility of tumors on standard MRI images (Flair MRI images) obtained from LM patients is even less (nearly 34%). There are little or no studies on diagnosis with LM tumor on MRI images [82].

Leptomeningeal surface does not always appear in brain MRI images of patients. However, MRI images have almost all kinds of information. MRI images of 42 patients in research group were examined and leptomeningeal surface was appeared in 35 patients' brain MRI images on the other hand leptomeningeal surface was not identified in seven patients' brain MRI images. Leptomeningeal surface were distinguished in the all patients' brain MRI images after image enhancement processing.

In another study carried out, 750 patients' records were selected in the pathology unit of Dicle University hospital which CSF examination has been obtained during the last decades.

Table 4.15 Demographic Table of patients' data in second study

	Number (%)	Mean age ± standard deviation
Male	12 (30.8)	50 (± 18.83)
Female	21 (69.2)	32 (± 17.529)
Sum	33 (100)	39 (± 19.453)

The selected patients' records were also examined in the radiology department and 33 patients were identified which had records in both the pathology unit and in the radiology department records. Cerebrospinal fluid analysis of these patients were reassessed with a particular pathologist from the pathology archives. In addition to this, these patients' MRI images were re-assessed with a particular radiologist in the radiology department and were reported.

The mean age of male in the second study is 50 and the mean age of female in the second study is 32. The mean age of all patients in second study is 39. 33 patients have been examined and the number of male is 12 and the number of female is 21 (Table 4.15).

Medical operation of LM cancer is almost impossible and the methods used for the treatment of LM cancer are respectively chemotherapy, radiotherapy and intra-CSF therapy or combination of these therapies. Some of infecting cancer cells on leptomeningeal layer falls into the CSF fluid and tumor can be determined by cytopathology analysis. Diagnosis of LM cancer is proportional to the amount of glucose rate in the CSF examination.

The amount of glucose rate in the CSF examination is less in suppurative meningitis, tuberculous meningitis, leukemic meningitis, metastases on the leptomeningeal layer and hypoglycemia (Table 4.16).

The reason why the definite results are obtained from CSF examination is to be counted cells in the CSF fluid.

Table 4.16 Changes the amount of glucose in the CSF fluid examination

High Glucose	Low Glucose
Higher glucose is not significant. It only shows to be hyperglycemia.	Bacterial meningitis
	Hyperglycemia
	SAK
	sarcoidosis

Series tests such as cells count and differential cells count are applied when CSF examination is done. These tests are applied to diagnose the dissemination of tumor on the brain and spinal cord which form CNS.

CSF examination is often used for the detection of cancers disseminated CNS such as LM cancer and also can be used for the detection of brain and spinal cord traumas. If the patient has symptoms such as severe headache, neck stiffness, hallucinations, confusion or dementia, remittances and flu-like symptoms which is prolonged or exacerbated, CSF examination should be requested.

CSF examination must be done in sterile tube and the received fluid must be accommodated in the proper nutrition. The main purpose of accommodation is to be performed the detailed analysis under a microscope after proper dyeing process. Cytological examination of the CSF fluid is made by taking the liquid on the slide to thoma. The received different amounts of liquid are examined in detail depending on the age of patients. If the patient is adult, the amount of CSF fluid is 0-5 mm^3, if the patient is a new-born, the amount of CSF fluid is 20 mm^3.

If the amount of cells in the CSF fluid is above 10 by mm^3, the sample has pathological feature. The increment of cells amount in the CSF fluid is defined as pleocytosis and also it is the sign of meningeal irritation. The measurement of CSF fluid should be carried out on an empty stomach and should be evaluated with a blood glucose measurement. The CSF glucose values are changed in connection with the blood glucose values through 1-3 hours. Normal CSF glucose values in the CSF fluid is 2/3 of blood glucose values and it does not exceed the amount of 45-80 mg/dl to 300 mg/dl. However, the glucose ratio between in the CSF fluid and in the blood of a new-born person is over 2/3.

The measurement of glucose in the CSF sample must be done immediately. The sample was centrifuged, stored at 4-20 C^o and fluoride was added in the sample.

In the Table 4.17, different ratios of four substance obtained in the CSF fluid indicate which diseases are corresponded. Lower glucose value and higher leukocyte and neutrophil values define the bacterial meningitis.

Table 4.17 The measurement and the provision of the substance located in the CSF fluid

Glucose	↓	Leukocyte	↑	Neutrophil	↑	=	Bacterial meningitis indicator
Glucose	↓	Leukocyte	↑	Lymphocytes	↑	=	Tuberculosis meningitis indicator
Glucose	N	Lymphocytes	↑			=	Viral meningitis indicator

Lower glucose value and higher leukocyte and lymphocytes values define tuberculosis meningitis. Normal glucose value and higher lymphocytes value define viral meningitis. Definitive diagnosis is given with CSF fluid examination because it is through carried out the exact number of values in the sample. The exact diagnosis of meningitis is according to definite measurement of CSF examination.

Cytological examination is obtained by needle aspiration of the tissue or by scraping or brushing on some tissue. Nuclear and cytoplasmic features of cells by individually or by groups are evaluated as a result of microscopic examination of the sample obtained at the end of the spreading process. Especially, the tumoral lesions presented pathological diagnostic approach “benign” or “malignant” is a non-invasive diagnostic methods and is a very important pathological process. The malignant cytology can be diagnosed the atypical character of malignant cell/cells and the benign cytology can be diagnosed the atypical cellular changes in smear-free obtained by the review of cytopathology. In particular, these findings provide important information for clinicians in the diagnosis and treatment of tumors.

REFERENCES

[1] Shah L.M. Salzman K.L. “Imaging of Spinal Metastatic Disease”, International Journal of Surgical Oncology, 2011

[2] Saleh H. Nordin J. “Improving Diagnostic Viewing of Medical Images using Enhancement Algorithms”, Journal of Computer Science 7 (12): 1831-1838, 2011

[3] Bai C. Shi H. Liu D. Zhu T. Hu Z. Li Q. “Gemcitabine plus oxaliplatin for the treatment of leptomeningeal metastases of non-small cell lung cancer: A case report and review of the literatüre” Oncology Letters 5: 1559-1561, 2013.

[4] Tepe S. “Contrast- FLAIR Versus Contrast- T1-Weighted Sequence of Magnetic Resonance Imaging for the Evaluation of Leptomeningeal Disease: Which one is Better?”. Archives of Neuropsychiatry 2012; 49: 108-113

[5] Giesel FL. Mehndiratta A. Essig M. (2010) “High-relaxivity contrast- magnetic resonance neuroimaging: a review”, European Radiology.

[6] Kaplan JG, DeSouza TG, Farkash A. et al., (1990) “Leptomeningeal metastases: comparison of clinical features and laboratory data of solid tumors, lymphomas and leukemias,” Journal of Neuro-Oncology, vol. 9, no. 3, pp. 225–229.

[7] Lee J.H., (2008) “Meningiomas: Diagnosis, Treatment, and Outcome”. Springer.

[8] Keen L.E. (2009) “Cerebrospinal Fluid in Clinical Practice”, Elsevier Inc.

[9] Frisk G, Svensson T, Backlund LM, Lidbrink E, Blomqvist P and Smedby KE. (2012) “Incidence and time trends of brain metastases admissions among breast cancer patients in Sweden.” Br J Cancer; 106: 1850-3.

[10] Boogerd W, Hart AA, van der Sande JJ, et al. (1991) “Meningeal carcinomatosis in breast cancer. Prognostic factors and influence of treatment.” Cancer; 67: 1685-95.

[11] Pfeffer MR, Wygoda M, Siegal T. (1988) “Leptomeningeal metastases treatment results in 98 consecutive patients.” Isr J Med Sci; 24: 611-8.

[12] Balducci L, Little DD, Khansur T, et al. (1984) "Carcinomatous meningitis in small cell lung cancer.” Am J Med Sci; 287:31-3.

[13] Eberth KJ. (1870) “Zur entwickelung des epitheliomas (cholesteatomas) der pia und der lung.” Virchows Arch.

[14] Posner, JB. (1995) “Neurologic complications of cancer.” Philadelphia: FA Davis.

[15] Pratt WK. (1989) “Digital image processing”, Prentice Hall.

[16] Deisenhammer F. Bartos A. Egg R. Gilhus N.E. Giovannoni G. Rauer S. Sellebjerg F. “Guidelines on routine cerebrospinal fluid analysis. Report from an EFNS task force”, European Journal of Neurology 2006.

[17] Malkin MG, Posner JB. (1987) "Cerebrospinal fluid tumor markers for the diagnosis and management of leptomeningeal metastases." Eur J Cancer Clin Oncol; 23(1):1–4.

[18] Davis FG, Dolecek TA, McCarthy BJ and Villano JL. (2012) "Toward determining the lifetime occurrence of metastatic brain tumors estimated from 2007 United States cancer incidence data." Neuro Oncol; 14: 1171-7.

[19] Brian J Scott, Santosh Kesari, (2013) "Leptomeningeal metastases in breast cancer", Am J Cancer Res;3(2):117-126

[20] Singh S.K. Leeds N.E. Ginsberg L.E. "MR Imaging of Leptomeningeal Metastases: Comparison of Three Sequences". AJNR Am J Neuroradiol 23:817–821, May 2002

[21] Nieuwenhuys, R.; Voogd, J.; Huijzen, C.V.; (2008). "The Human Central Nervous System A Synopsis and Atlas". Spinger, 967 p.

[22] Decimo I, Fumagalli G, Berton V, Krampera M, Bifari F.; (2012) "Review Article Meninges: from protective membrane to stem cell niche". Am J Stem Cell

[23] Tortora G.J., Derrickson B.H., (2015) "Boundless alternative to Principles of Anatomy and Physiology" 13th edition

[24] Noback C.R., Ruggiero D.A., Demarest R.J., Strominger N.L., (2005) "The Human Nervous System: Structure and Function", Humana Press Inc. pp 89-99

[25] www.boundless.com/physiology/central-nervous-system-cns/protection-of-the-brain/meninges/ access time 04/04/2015

[26] Hernandez-Ramos FJ, Serrano-Castro PJ. (1996) "Deafness from leptomeningeal metastasis." Neurologia; 11:344.

[27] Drappatz, J.; Batchelor, T. (2009) "Leptomeningeal metastasis". American society of clinical oncology educational book; p. 100-105.

[28] Kokkoris CP. (1983) "Leptomeningeal carcinomatosis. How does cancer reach the pia-arachnoid?" Cancer; 51:154–160.

[29] Bomgaars L, Chamberlain MC, Poplack DG, Blaney SM. (2002) "Leptomeningeal Metastases" Page 375

[30] Leal, T. Chang, J. E. Mehta, M. Robins, H. I. (2011)"Leptomeningeal Metastasis: Challenges in Diagnosis and Treatment" Curr Cancer Ther Rev.

[31] Chamberlain MC, Balm M, and Hammack J, (1997) "Carcinomatous meningitis" Archives of Neurology, vol. 54, no. 1, pp. 16–17.

[32] Norden AD, Wen PY, Kesari S. (2005) "Brain metastases." Curr Opin Neurol; 18:654.

[33] Omar, AI. Mason, WP. (2009) "Neurologic complications of cancer." 2nd edition. New York: Oxford University Press, Inc; p. 240-281.

[34] Lai R, Dang CT, Malkin MG and Abrey LE. (2004) "The risk of central nervous system metastases after trastuzumab therapy in patients with breast carcinoma." Cancer; 101: 810-816.

[35] Lower EE, Drosick DR, Blau R, Brennan L, Danneman W and Hawley DK. (2003) “Increased rate of brain metastasis with trastuzumab therapy not associated with impaired survival.” Clin Breast Cancer; 4: 114-9.

[36] LM DeAngelis and JB Posner, (2009) “Neurologic Complications of Cancer”, Neurocritical Care 10:149.

[37] Zairi FKN, Rodrigues I, Baranzelli M, Andre C, Dubois F, Devos P, Faivre-Pierret M, Assaker R, Bonneterre J, Le Rhun E. (2012) “Prospective follow-up of a cohort of 112 patients with leptomeningeal metastases of breast cancer recruited from 2007-2011: Prognostic factors”; Journal of clinical oncology: official journal of the American Society of Clinical Oncology; 30.

[38] http://emedicine.medscape.com/article/338239-overview access time 04/04/2015

[39] Nussbaum ES, Djalilian HR, Cho KH, Hall WA. (1996) “Brain metastases. Histology, multiplicity, surgery, and survival. Cancer”; Cancer; 78:1781-1788.

[40] Russ JC. (1998) “The Image Processing Handbook”. CRC Press,

[41] “Leptomeningeal Carcinomatosis Imaging”, http://emedicine.medscape.com/article/341389-overview, access time 04/04/2015

[42] Metwally Y, (2013) “Dissemination of Primary CNS Tumors“ p.419.

[43] Schold SC, Wasserstrom WR, Fleisher M, Schwartz MK, Posner JB. (1980) “Cerebrospinal fluid biochemical markers of central nervous system metastases.” Ann Neurol; 8:597.

[44] http://www.norolojiklinigi.info/bos.html access time 04/04/2015

[45] Tatlı B. (2008) “Püf Noktası Beyin Omurilik Sıvısının Değerlendirilmesi” Çocuk Dergisi 8(4):261-262

[46] Patchell RA, Tibbs PA, Walsh JW, et al. (1990) “A randomized trial of surgery in the treatment of single metastases to the brain.” N Engl J Med; 322:494.

[47] Chamberlain MC. (2000) “Neoplastic meningitis: a guide to diagnosis and treatment”; Curr Opin Neurol; 13:641.

[48] Chamberlain MC, Sandy AD, Press GA. (1990) “Leptomeningeal metastasis: A comparison of gadolinium- MRI and contrast- ct of the brain.” Neurology. 40:435–438.

[49] Schniederjan MJ, Alghamdi S, Castellano-Sanchez A, Mazewski C, Brahma B, Brat DJ, et al. (2013) “Diffuse leptomeningeal neuroepithelial tumor: 9 pediatric cases with chromosome” The American Journal of Surgical Pathology.

[50] Groves M. (2008) “Leptomeningeal metastases: Still a challenge” ASCO educational book. 80–87.

[51] Kleinfeld K, Peters WH, Stephenson C, Azar NJ. (2013) “Leptomeningeal metastasis from occult signet-ring cell colon adenocarcinoma presenting with isolated headache.” J Clin Neurosci; 20(6):890-2.

[52] Rydberg J, et al. (2000) “Multisection CT:Scanning Techniques and Clinical Applications”, Radiographics, 1787-1806

[53] Turner R, Jones T, (2003) “Techniques for imaging neuroscience.” British Medical Bulletin 65: 3-20

[54] N. Shastry Akella, Donald B. Twieg, Tom Mikkelsen, Fred H. Hochberg, Stuart Grossman, Gretchen A. Cloud, and L. Burt Nabors, (2004) “Assessment of Brain Tumor Angiogenesis Inhibitors Using Perfusion Magnetic Resonance Imaging: Quality and Analysis Results of a Phase I Trial”, Journal of Magnetic Resonance Imaging 20:913–922

[55] Daldrup H, Shames DM, Wendland M, et al. (1998) “Correlation of dynamic contrast magnetic resonance imaging with histological tumor grade: comparison of macromolecular and small-molecular contrast media.” Neuroradiology; 28:67–78.

[56] http://brain101.info/Neuro_Imaging.pdf access time 04/04/2015

[57] Rosen Y, (2007) “The recent advances in magnetic resonance neurospectroscopy.” Neurotherapeutics, 27(3):330-45

[58] Kwan-Hoong Ng, Ahmad AC, Nizam MS, Abdullah BJJ, (2003) “Magnetic Resonance Imaging: Health Effects and Safety”, Proceedings of the International Conference on Non-Ionizing Radiation at UNITEN (ICNIR2003) Electromagnetic Fields and Our Health 20th – 22nd

[59] http://www.barnabashealth.org/hospitals/community_medical/radiology/mri.html access time 04/04/2015

[60] http://peds.stanford.edu/Rotations/radiology/documents/MRI_SAFETY.pdf access time 04/04/2015

[61] http://www.samc.org/index.php/diagnostic-imaging-menu/home/mri access time 04/04/2015

[62] Weissman B.N.W, (2009) “Imaging of Arthritis and Metabolic Bone Disease”; MOSBY

[63] http://www.diffen.com/difference/CT_Scan_vs_MRI access time 04/04/2015

[64] Kesari S, Batchelor TT. (2003) “Leptomeningeal metastates.” Neurol Clin, 21: 25-66.

[65] Glantz MJ, Cole BF, Recht L, et al. (1998) "High-dose intravenous methotrexate for patients with nonleukemic leptomeningeal cancer: Is intrathecal chemotherapy necessary?” J Clin ncol. 16:1561–1567.

[66] Hennann B, Hultenschmidt B, Sautter-Bibl ML. (2001) “Radiotherapy of the neuroaxis for palliative treatment of leptomeningeal carcinomatosis.” Strahlenther Onkol. 177:195–199.

[67] Mehta M, Bradley K. (2005) “Radiation therapy for leptomeningeal cancer.” Cancer Treatment and Research. 125:147–158.

[68] Glantz MJ, LaFollette S, Jaeckle KA, et al. (1999) "Randomized trial of a slow-release versus a standard formulation of cytarabine for the intrathecal treatment of lymphomatous meningitis"; J Clin Oncol.; 17:3110–3116.

[69] Davis LE. King MK. Schultz JL. (2005) "Fundamentals of Neurologic Disease", The Journal of Spinal Cord Medicine.

[70] Gonzalez RC. (2009) "Digital Image Processing", Second Edition. Prentice Hall

[71] Maini R. Aggarwal H. (2010) "A Comprehensive Review of Image Enhancement Techniques", Journal of Computing, Volume 2, Issue 3.

[72] Jain AK. (1989) "Fundamentals of Digital Image Processing", Englewood Cliffs, NJ: Prentice Hall.

[73] Haralick RM, Shapiro LG, (1992) "Computer and Robot vision", Vol-1, Addison-Wesley Pub. Co

[74] Solomon C. Breckon T. (2011) "Fundamentals of Digital Image Processing - A Practical Approach with Examples in Matlab" Wiley-Blackwell.

[75] Schellinger PD, Meinck HM, Thron A. (1999) "Diagnostic accuracy of MRI compared to CCT in patients with brain metastases" J Neurooncol; 44:275.

[76] Tosoni A, Ermani M, Brandes AA. (2004) "The pathogenesis and treatment of brain metastases: a comprehensive review"; Crit Rev Oncol Hematol; 52:199.

[77] Jemal A, Siegel R, Xu J, Ward E. (2010) "Cancer statistics"; CA Cancer J Clin; 60:277

[78] Schumacher M, Orszagh M. (1998) "Imaging techniques in neoplastic meningiosis"; J Neurol Oncol.;38:111–120.

[79] Sze G, Soletsky S, Bronen R, et al. (1989) "MR imaging of the cranial meninges with emphasis on contrast enhancement and meningeal carcinomatosis"; AJR Am J Roentgenol;153:1039 –1049.

[80] Yousem DM, Patrone PM, Grossman RI. (1990) "Leptomeningeal Metastases: MR Evaluation", Journal of Computer Assisted Tomography 14(2):255-261.

[81] Collie DA, Brush JP, Lammie GA, Granti R, Kunklers I, Leonards R, Gregors A, Sellar RJ, (1999) "Imaging Features of Leptomeningeal Metastases", Clinicol Radiology 54, 765-771

[82] Singh SK, Agris JM, Leeds NE, Ginsberg LE, (2000) "Intracranial Leptomeningeal Metastases: Comparison of Depiction at FLAIR and Contrast-MR Imaging“, Radiology.

APPENDICES

APPENDIX A

DİCLE ÜNİVERSİTESİ TIP FAKÜLTESİ GİRİŞİMSEL OLMAYAN KLİNİK ARAŞTIRMALAR ETİK KURULU

DİCLE UNIVERSITY MEDICAL FACULTY ETHICS COMMITTEE FOR NONINTERVENTIONAL STUDIES

85

KARAR

Prof. Dr. Abdurrahman IŞIKDOĞAN, Prof. Dr. Sadık KARA, Öğr. Gör. Mehmet GÜL, Yrd. Doç. Dr. Cemil GOYA, Uzm. Dr. Yusuf YARAR araştırmacılar tarafından planlanan "Leptomeningeal metastaz hastalarının MRI görüntülerinin incelenerek erken tanı konulması" başlıklı araştırmaya *Dicle Üniversitesi Tıp Fakültesi Etik Kurul'u* tarafından toplantıda hazır bulunan üyeler tarafından oy birliği ile onay verilmiştir.

Klinik araştırma tamamlanıp yayın aşamasına geldiğinde, yayına sunulan bildiri veya makalenin bir örneğinin Etik Kurul'a verilmesi zorunludur.

DECISION

The project titled as "Examination of mri images of leptomeningeal metastasis cancer patients for early diagnosis" planned Abdurrahman IŞIKDOĞAN, Sadık KARA, Mehmet GÜL, Cemil GOYA, Yusuf YARAR has been approved by Ethics Committee of Dicle University Faculty of Medicine.

Oturum No (Meeting number) :	Tarih (Date): 23.01.2015	Saat (Hour): 13:00-15:00
KURUL BAŞKANI (CHIEF)	Prof. Dr. Aydın ECE	

KURUL ÜYELERİ / MEMBERS

	ÜNVANI	ADI-SOYADI	KURUMU	BRANŞI	İMZA
1	Prof. Dr.	Aydın ECE	Dicle Üniversitesi Tıp Fakültesi	Çocuk Sağlığı ve Hst.	
2	Yrd. Doç. Dr.	İbrahim KAPLAN	Dicle Üniversitesi Tıp Fakültesi	Biyokimya	
3	Prof. Dr.	Süleyman GÖREN	Dicle Üniversitesi Tıp Fakültesi	Adli Tıp	
4	Yrd. Doç. Dr.	İlker KELLE	Dicle Üniversitesi Tıp Fakültesi	Tıbbi Farmakoloji	
5	Doç.Dr.	A. Çetin TANRIKULU	Dicle Üniversitesi Tıp Fakültesi	Göğüs Hast.	
6	Doç. Dr.	Abdullah BÖYÜK	Dicle Üniversitesi Tıp Fakültesi	Genel Cerrahi	
7	Yrd. Doç. Dr.	İsmail YILDIZ	Dicle Üniversitesi Tıp Fakültesi	Biyoistatistik	
8	Doç. Dr.	Uğur FIRAT	Dicle Üniversitesi Tıp Fakültesi	Patoloji	
9	Yrd. Doç. Dr.	Orhan ATEŞ	Dicle Üniversitesi İlahiyat Fakültesi	Temel İslam Bilimleri	
10	Doç. Dr.	Mehmet Uğur ÇEVİK	Dicle Üniversitesi Tıp Fakültesi	Nöroloji	
11	Avukat	Şahhanım KAPLAN	Dicle Üniversitesi Hastaneleri Başhekimlik	Avukat	

Dicle Üniversitesi Tıp Fakültesi Dekanlık Binası Zemin Kat 21280 Kampüs/DİYARBAKIR
Telefon:+90.412 . 248 80 01-16/4631 Faks:+90.412. 248 84 40 kuruletikdiyar@gmail.com

DİCLE ÜNİVERSİTESİ TIP FAKÜLTESİ GİRİŞİMSEL OLMAYAN KLİNİK ARAŞTIRMALAR ETİK KURULU

DİCLE UNIVERSITY MEDICAL FACULTY ETHICS COMMITTEE FOR NONINTERVENTIONAL STUDIES

337

KARAR

Doç. Dr. Uğur FIRAT, Öğr. Gör. Mehmet GÜL, Prof. Dr. Sadık KARA, Prof. Dr. Abdurrahman IŞIKDOĞAN, Dr. Yusuf YARAR, Yrd. Doç. Dr. Cihad HAMİDİ araştırmacılar tarafından planlanan "Leptomeningeal metastaz hastalarının magnetic resonance imaging (MRI) görüntüleri ile bu hastalara ait beyinomurilik sıvısı patolojik değerlendirme sonuçlarının karşılaştırılması" başlıklı araştırmaya *Dicle Üniversitesi Tıp Fakültesi Etik Kurul'u* tarafından toplantıda hazır bulunan üyeler tarafından oy birliği ile onay verilmiştir.

Klinik araştırma tamamlanıp yayın aşamasına geldiğinde, yayına sunulan bildiri veya makalenin bir örneğinin Etik Kurul'a verilmesi zorunludur.

DECISION

The project titled as "Comparison of leptomeningeal metastases cancer patients' magnetic resonance imaging (MRI) with cerebrospinal fluid pathological examination results" planned Uğur FIRAT, Mehmet GÜL, Sadık KARA, Abdurrahman IŞIKDOĞAN, Yusuf YARAR, Cihad HAMİDİ has been approved by Ethics Committee of Dicle University Faculty of Medicine.

Oturum No (Meeting number) :	Tarih (Date): 30.07.2015	Saat (Hour): 13:00-15:00
KURUL BAŞKANI (CHIEF)	Prof. Dr. Aydın ECE	

KURUL ÜYELERİ / MEMBERS

	ÜNVANI	ADI-SOYADI	KURUMU	BRANŞI	İMZA
1	Prof. Dr.	Aydın ECE	Dicle Üniversitesi Tıp Fakültesi	Çocuk Sağlığı ve Hst.	
2	Yrd. Doç. Dr.	İbrahim KAPLAN	Dicle Üniversitesi Tıp Fakültesi	Biyokimya	
3	Prof. Dr.	Süleyman GÖREN	Dicle Üniversitesi Tıp Fakültesi	Adli Tıp	
4	Yrd. Doç. Dr.	İlker KELLE	Dicle Üniversitesi Tıp Fakültesi	Tıbbi Farmakoloji	
5	Doç.Dr.	A. Çetin TANRIKULU	Dicle Üniversitesi Tıp Fakültesi	Göğüs Hast.	
6	Doç. Dr.	Abdullah BÖYÜK	Dicle Üniversitesi Tıp Fakültesi	Genel Cerrahi	
7	Yrd. Doç. Dr.	İsmail YILDIZ	Dicle Üniversitesi Tıp Fakültesi	Biyoistatistik	
8	Doç. Dr.	Uğur FIRAT	Dicle Üniversitesi Tıp Fakültesi	Patoloji	
9	Doç. Dr.	Orhan ATEŞ	Dicle Üniversitesi İlahiyat Fakültesi	Temel İslam Bilimleri	
10	Doç. Dr.	Mehmet Uğur ÇEVİK	Dicle Üniversitesi Tıp Fakültesi	Nöroloji	
11	Avukat	Şahhanım KAPLAN	Dicle Üniversitesi Hastaneleri Başhekimlik	Avukat	

Dicle Üniversitesi Tıp Fakültesi Dekanlık Binası Zemin Kat 21280 Kampüs/DİYARBAKIR
Telefon:+90.412 . 248 80 01-16/4631 Faks:+90.412. 248 84 40 kuruletikdiyar@gmail.com

APPENDIX B

Bit-Plane Slicing Method Code

```
I=imread('saliha bozdemir 1.jpg');

A = I * 0;

[w h]=size(x);

for i=1:w

    for j=1:h

        b=bitget(I(i,j),1); % if this value is changed, different images are obtained

        y(i,j)=bitset(y(i,j),8,b);

    end

end

Figure, imshow(x);

Figure, imshow(y);

imwrite(A, 'saliha bozdemir 1-BPS.jpg');
```

Contrast Stretching Method Code

```
I = imread(' saliha bozdemir 1.jpg');

lim = stretchlim(I, 0.18);

J = imadjust(I, lim, []);

Figure, imshow(I), Figure, imshow(J);

imwrite(J, 'saliha bozdemir 1-CT.jpg');
```

Gray-Level Slicing Method Code

```
I=imread('saliha bozdemir 1.jpg');
A = I;
B = I;
[w h]=size(I);
for i=1:w
    for j=1:h
        if I(i,j)>=90 && x(i,j)<=255 A(i,j)=255;
        else A(i,j)=0;
        end
    end
end
Figure, imshow(B), Figure, imshow(I);
imwrite(A, 'saliha bozdemir 1-GLS.jpg');
```

Logarithmic Transformation Method Code

```
h = imread('şeyhmus elçin-2.jpg');

g = 0.15 * log(1 + double(h));

imshow(h), Figure, imshow(g);

imwrite(g, 'şeyhmus elçin-2-LT.jpg');
```

Negative Transformation Method Code

```
I = imread('şeyhmus elçin-2.jpg');

g = imcomplement(I);

imshow(I), Figure, imshow(g);

imwrite(g,'şeyhmus elçin-2-NT.jpg');
```

Power-Law Transformation Method Code

```
clear all
close all
I=imread('şeyhmus elçin-2.jpg');
A=rgb2gray(I);
A=im2double(A);
[m n] = size(A);
c = 2;
g =[0.5];
for r=1:length(g)
for p = 1 : m
   for q = 1 : n
       B(p, q) = c * A(p, q).^ g(r);
   end
end
Figure, imshow(I3);
title('Power-law transformation');
xlabel('Gamma='), xlabel(g(r));
imwrite(B,'şeyhmus elçin-2-PL.jpg');
end
```

Thresolding Method Code

```
I = imread('şeyhmus elçin-2.jpg');

level = graythresh(I);

BW = im2bw(I,level);

imshow(BW);

imwrite(BW,'şeyhmus elçin-2-Thr.jpg');
```

Histogram Processing Method

```
clc; clear all;
img = imread('saliha bozdemir 1.jpg');
 if(size(img,3) > 1)
    img = rgb2gray(img);
end;
img = imresize(img,[256 256],'bicubic');
max_r = size(img,1);
max_c = size(img,2);
histogram = zeros([1 256]);
cumulative_hist = zeros([1 256]);
for r=1:max_r
    for c=1:max_c
        for count=1:256
            if(img(r,c) == count-1)
                histogram(count) = histogram(count) + 1;
                break;
            end
        end
    end
end
current_value = 0;
for count=1:256
    current_value = current_value + histogram(count);
```

```
    cumulative_hist(count) = current_value;
end
normalized_hist = zeros([1 256]);
cdf_min = min(cumulative_hist);
for count=1:256
    normalized_hist(count) = cumulative_hist(count) - cdf_min;
    normalized_hist(count) = normalized_hist(count) / ( (max_r*max_c) - cdf_min);
    normalized_hist(count) = round(normalized_hist(count) * 255);
end
equalized_image = zeros([max_r max_c]);
for r=1:max_r
    for c=1:max_c
        for count=1:256
            if(img(r,c) == (count-1))
                equalized_img(r,c) = normalized_hist(count);
                break;
            end
        end
    end
end
subplot(2,2,1)
imshow(img);
title('Original Image');
subplot(2,2,2);
imhist(img);
```

```
title('Histogram Original Image');

subplot(2,2,3);

imshow(uint8(equalized_img));

title(' Image');

H=uint8(equalized_img);

subplot(2,2,4);

imhist(H);

title('Histogram of  Image');
```

CURRICULUM VITAE

Name Surname: Mehmet GÜL

Place and Date of Birth: 24/03/1982 – Diyarbakır

Address: Bağcılar mahallesi 1204 sokak Seçkin City Sitesi A blok Kat:5 No:12 Bağlar/Diyarbakır

E-Mail: mehmetgul@ymail.com

B.Sc.: Middle East Technical University – Computer Education and Instructional Technology

M.Sc.: Fırat University – Computer Engineering

Professional Experience:

- **02/2006 – 12/2009:** Computer Teacher – MEB
- **12/2009 –** Lecturer – Dicle University

List of Publications:

- **Gül M**. Kara S. Işıkdoğan A. Yarar Y. Olgaç M. "Leptomeningeal Metastaz Hastalarının MR Görüntülerinin Histogram Eşitleme Metodu ve Logaritmik Dönüşüm Metodu ile İyileştirilmiş Sonuçlarının Kıyaslanması". Tıp Teknolojileri Ulusal Kongresi – TıpTekno 2014
- **Gul M**. Kara S. Işıkdoğan A. Yarar Y. Olgac M. Yıldız İ. "Diagnosis of Leptomeningeal Metastases Disease with MRI images by Logarithmic Transformation Method". BME 2014 Biomedical Engineering International Conference. 2014
- **Gül M**. Kara S. Işıkdoğan A. Yarar Y. ve Yıldız İ. "Leptomeningeal Melanomatosis Hastalarının MR Görüntülerinin PowerLaw Dönüşüm Metodu ile İyileştirilmesi". Tıp Teknolojileri Ulusal Kongresi – TıpTekno 2015
- **Gül M**. Kara S. Işıkdoğan A. ve Fırat U. "Leptomeningeal Karkinomatosis Hastalarının İyileştirilmiş MR Görüntüleri ile Patoloji Sonuçlarının Kıyaslanması". Tıp Teknolojileri Ulusal Kongresi – TıpTekno 2015

PUBLICATIONS/PRESENTATIONS ON THE THESIS

- **Gul M**. Kara S. Işıkdoğan A. and Yarar Y. "Diagnosis of Leptomeningeal Metastases Disease in MRI Images by Using Image Enhancement Methods". International Arab Journal of Information Technology (IAJIT), Vol. 14, No. 6, November 2017.